DAMAGE DETECTION IN STRUCTURES USING VIBRATION MEASUREMENTS

A THESIS SUBMITTED TO
THE GRADUATE SCHOOL OF NATURAL AND APPLIED SCIENCES
OF
THE MIDDLE EAST TECHNICAL UNIVERSITY

BY

MUSTAFA ÖZGÜR AYDOĞAN

IN PARTIAL FULLFILLMENT OF THE REQUIREMENTS FOR THE DEGREE OF
MASTER OF SCIENCE
IN
THE DEPARTMENT OF MECHANICAL ENGINEERING

DECEMBER 2003

Approval of Graduate School of Natural and Applied Sciences

_____
Prof. Dr. Canan ÖZGEN
Director

I certify that this thesis satisfies all requirements as a thesis for Degree of Master of Science.

_____
Prof. Dr. Kemal İDER
Head of the Department

This is to certify that we have read this thesis and that in our opinion it is fully adequate, in scope and quality, as a thesis for the degree of Master of Science.

_____
Prof. Dr. H. Nevzat ÖZGÜVEN
Supervisor

Examining Comitte Members

Prof. Dr. Y. Samim ÜNLÜSOY (Chairman)   _____

Prof. Dr. H. Nevzat ÖZGÜVEN   _____

Prof. Dr. Mehmet ÇALIŞKAN   _____

Prof. Dr. Kemal ÖZGÖREN   _____

Dr. Mutlu Devrim CÖMERT   _____

ABSTRACT

DAMAGE DETECTION IN STRUCTURES USING VIBRATION MEASUREMENTS

AYDOĞAN, Mustafa Özgür

M.S., Department of Mechanical Engineering

Supervisor: Prof. Dr. H. Nevzat ÖZGÜVEN

December 2003, 89 Pages

Cracks often exist in structural members that are exposed to repeated loading, which will certainly lower the structural integrity. A crack on a structural member introduces a local flexibility which is a function of the crack depth and location. This may cause nonlinear dynamic response of the structure.

In this thesis, a new method is suggested to detect and locate a crack in a structural component. The method is based on the fact that nonlinear response of a structure with a crack will be a function of the crack location and crack magnitude. The method suggested is the extension of a recently developed technique for identification of non-linearity in vibrating multi degree of freedom

system. In this method, experimentally measured receptances at different forcing levels are used as input, and the existence and location of a nonlinearity are sought.

In order to validate the method, simulated experimental data is used. Characteristics of a cracked beam are simulated by using experimentally obtained analytical expressions, given in the literature. The structure itself is modelled by using finite element method. Several case studies are performed to test and demonstrate the applicability, efficiency and sensitivity of the method suggested. The effect of crack depth on nonlinear system response is also studied in numerical examples.

Keywords: Structural Dynamics, Crack Detection, Crack Identification, Nonlinear Identification, Nonlinear Vibrations, Non-Linear Dynamics.

ÖZ

TİTREŞİM ÖLÇÜMLERİNİ KULLANARAK YAPILARDA HASAR TESBİTİ

AYDOĞAN, Mustafa Özgür

Yüksek Lisans, Makine Mühendisliği Bölümü

Tez Danışmanı: Prof. Dr. H. Nevzat ÖZGÜVEN

Aralık 2003, 89 Sayfa

Çatlaklar, genellikle, tekrarlanan yüklemelere maruz kalan yapı elemanlarında, yapısal bütünlüğü bozan bir etken olarak ortaya çıkar. Yapısal bir eleman üzerindeki bir çatlak, bulunduğu bölgede, çatlağın yeri ve derinliğine bağlı fazladan bir esneklik oluşturur. Bu da, söz konusu yapıda doğrusal olmayan dinamik tepkilere neden olur.

Bu tezde, yapılardaki hasarların tesbiti ve yerinin belirlenmesi için yeni bir yöntem önerilmiştir. Bu yöntem, içinde çatlak bulunduran yapının doğrusal olmayan tepkilerinin, söz konusu çatlağın yeri ve büyüklüğünün bir fonksiyonu olacağı gerçeğine dayanır. Önerilen yöntem, çok serbestlik dereceli titreşen

sistemlerde doğrusal olmayan elemanların tanılanması için, önceki çalışmalarda geliştirilen bir yöntemin geliştirilmiş halidir. Bu yöntemde, değişik kuvvet düzeylerinde elde edilen deneysel tepki fonksiyonları girdi olarak kullanılarak, söz konusu yapıdaki hasarın varlığı ve yeri araştırılmaktadır.

Yöntemin geçerliliğinin saptanması için, deneysel veriler yerine teorik olarak hesaplanmış değerler kullanılmıştır. Üzerinde çatlak bulunan yapının modellenmesinde, çeşitli kaynaklarda verilen ve deneysel çalışmalar sonucunda elde edilen analitik ifadeler kullanılmıştır. Yapının kendisi, sonlu eleman tekniği kullanılarak modellenmiştir. Önerilen yöntemin uygulanabilirliğini, verimliliğini ve hassasiyetini göstermek için çeşitli örnek uygulamalar incelenmiştir. Çatlağın derinliğinin, doğrusal olmayan sistem tepkelerine etkisi de çeşitli sayısal çözümlemelerle araştırılmıştır.

Anahtar Kelimeler: Yapısal Dinamik, Çatlak Tesbiti, Çatlak Tanılanması, Doğrusal Olmayan Sistem Tanılanması, Doğrusal Olmayan Titreşimler

"If you have built castles in the air, your work need not be lost;

there is where they should be.

Now put the foundations under them".

Henry David Thoreau.

(1817~1862)

ACKNOWLEDGEMENTS

TABLE OF CONTENTS

LIST OF FIGURES

NOMENCLATURE

a   : Depth of the crack

b   : Width of the cross section of beam

c   : Flexibility coefficient

$[C]$: Global damping matrix

E   : Modulus of elasticity

$\{f\}$: Vector of external forcing

$\{F\}$: Complex amplitude vector of external forces

h   : Depth of cross section of beam

$[I]$: Identity matrix

$[K]$: Global stiffness matrix

$[K]_{ce}$: Stiffness matrix of cracked finite beam element

$[K]_{ue}$: Stiffness matrix of uncracked finite beam element

K_I : Stress intensity factor for opening type of crack

K_{II} : Stress intensity factor for sliding type of crack

K_{III} : Stress intensity factor for tearing type of crack

l   : Length of beam

L   : Length of a finite beam element

m_1 : Generic stiffness value

m_2 : Generic stiffness value

$[M]$: Global mass matrix

$[M]_e$: Mass matrix of finite beam element

n_{kj} : Nonlinear restoring force element

$\{N\}$: Vector of internal nonlinear forces

$\{\mathbb{N}\}$: Complex amplitude vector of internal quasi-linear forces

q   : Generalized displacement vector

Q   : Complex amplitude vector of external forces (finite element)

s   : Inverse crack depth ratio

t   : Time variable

u_i : i-th displacement coordinate for a finite beam element

W   : Strain energy

$\{x\}$: Vector of generalized coordinates

$\{X\}$: Complex amplitude vector of displacements

y_{kj} : Inter-coordinate displacement

Y_{kj} : Complex amplitude of the inter-cordinate displacement y_{kj}

$[Z]$: Dynamic stiffness matrix

$[\alpha]$: Linear receptance matrix

$[\Delta]$: Non-linearity matrix.

$[\Xi]$: Mass normalized mode shape matrix

θ_i : i-th rotational coordinate of a finite beam element

$[\Theta]$: Pseudo-receptance matrix

ζ_i : i^{th} modal damping ratio

ρ : Mass density

δ_{ir} : Kronecker delta function

δ : Clearance

$[T]$: Transformation matrix

ν : Poisson's ratio

ψ : Generic angle

ω_{ni} : i^{th} natural frequency

$\{\omega_n\}$: Vector of natural frequencies

CHAPTER 1

INTRODUCTION

Cracks are generally the main reasons of sudden structural failures during machine operations. They may cause serious damage or injury; therefore detecting damage in structural components at the earliest possible stage has become an important aspect in today's engineering. There are various techniques in crack detection. One of the techniques in non destructive detection and locating of cracks is the use of vibration response of the structures.

The presence of a crack in a structural component leads to a local reduction in stiffness and an increase in damping which will affect its vibration response. The crack opens and closes in time depending on the vibration amplitude. This makes the system nonlinear. However, a damage in a structure, in general, may introduce linear or nonlinear modification to the structure [1]. If a linear-elastic structure remains linear-elastic after damage is introduced, then

1

this is said to be a linear damage. In this case, the vibratory response of the damaged structure can still be modeled by a linear equation of motion. On the other hand, if linear-elastic structure begins to behave in a nonlinear manner after the damage is introduced, then it is called nonlinear damage. A fatigue crack that subsequently opens and closes under harmonic excitation is a kind of nonlinear damage.

Damage identification methods are classified according to the type of measured data and the technique to gather that data. They are mainly based upon the shifts in natural frequencies or dynamically measured flexibilities and changes in mode shapes. Such changes are usually detected by matrix update or stiffness error methods and neural network methods which compare and contrast the damaged and the undamaged specimens.

Rytter [2] defined four levels of damage identification as:

- Determination of the damage that is present in the structure, level 1,
- Determination of the geometric location of the damage, level 2,
- Quantification of the severity of the damage, level 3,
- Prediction of the remaining service life of the structure, level 4.

There are two types of problems related to damaged structures. Namely,

forward (direct) problem and inverse problem. The forward problem is to find out the effect of damages on the structural dynamic properties. For example, calculating natural frequency shifts of a structural component due to a known type of damage. In such problems, damage is modeled mathematically, and then the measured natural frequencies are compared to the predicted ones to determine the damage. This problem can be classified as level 1 damage identification [1].

The inverse problem, on the other hand, consists of detecting, locating and quantifying damages present on a structural component. For example, calculating damage parameters, such as crack length and location. This problem can be classified as level 2 or level 3 damage identification [1].

Many studies in the literature use open crack models and calculate the change in natural frequency in order to detect the presence of cracks. But, the assumption that cracks are always open during vibration is not realistic. In order to overcome this unrealistic assumption, in some studies which are mentioned in the next chapter, cracks are modelled with bilinear behavior. In this approach, damaged structure is associated with two flexibility values: one for the state of crack open and the other for the crack close. This approach does not account for the crack surface interference during fatigue, and furthermore the crack is assumed to have two perfectly flat surfaces and exist only in the fully open or

fully closed states. In reality, however, the roughness of the fracture surface, corrosion debris in the crack, plastic deformation left in the wake of a propagating crack and hydraulic wedging produced by oil trapped in the crack may lead to partial crack closure [3]. Therefore, the flexibility of the damaged component having a crack will change continuously with time.

CHAPTER 2

LITERATURE SURVEY AND PRESENT STUDY

2.1 Literature Survey

Qian et al. [4] developed a FE cracked beam model for a cantilever beam with an edge crack. They proposed a simple method for determining the crack position, which is based on the relationship between the crack and eigenvalues of the beam.

Rizos et al. [5] investigated the flexural vibrations of a cantilever beam with a rectangular cross-section having a transverse surface crack which is modelled as a massless rotational spring. They also assumed that the crack is fully open and has uniform depth. As an experimental study, they forced the beam by a harmonic exciter to vibrate at one of the natural modes of vibration and measured the amplitudes at two positions.

Ostachowicz and Krawczuk [6] modelled a beam having an open and closed single-sided crack by triangular disk finite elements with two dof at each node. They showed the importance of two dimensionless ratios (the ratio of the distance along the beam from a reference point to the point where the crack is located to the beam's total length, and the ratio of crack's depth to the beam's depth) in determining the crack location and magnitude. Then, they investigated the effects of open double-sided and single-sided cracks on the natural frequencies of the flexural vibrations of a cantilever beam [7]. In this work, stiffness at crack location is calculated by using structural intensity factors at the crack location.

Kam and Lee [8] developed a procedure for identifying a crack in a structure. In this study, the structure is discretized into a set of elements and the crack is assumed to be located within one of the elements. Strain energy equilibrium equation for the cracked structure is derived based on the conservation of energy for estimating the crack size.

Armon et al. [9] developed a method for detecting and locating cracks in a beam. They formulated the fractional eigenvalue shifts for four modes of a clamped-free beam and plotted curves of these shifts as a function of position onto the same axes. They defined regions on this plot that were specified by a rank ordering operation of the fractional eigenvalue shifts. Furthermore, they performed experiments on cracked and uncracked beams to find the change in natural

frequencies and rank-ordered these data as well. By matching between rank orders of the data and plot, the cracks were located along the length of the beam.

Narkis [10] studied the effects of damages on the structural dynamic characteristics. This study was limited to uniform cantilever and simply supported beam.

Sundermeyer and Weaver [11] modelled a cracked vibrating beam to determine crack location, depth and opening load of it. They modeled the crack by a rotational spring the compliance of which is calculated basing on linear elastic fracture mechanics and Castigliano's Theorem. Two seperate beam model were formed for open-crack and close-crack cases by utilizing Bernoulli-Euler Beam Equation. For open-crack case, they broke-up the beam into two sections and considered boundary conditions of displacement, bending moment, shear and continuity at the crack location. For close-crack case, the beam was treated as a continuous Bernoulli beam. They illustrated the dependence of frequency spectrum on crack position for a variety of crack sizes. These illustrations were used to extract the crack parameters. They also investigated the effect of static load on crack signature.

Dimarogonos [12] presented a state of art review of various methods in tackling the cracked structure problem. In this study, cracked beams, plates,

turbine rotors, turbine blades, pipes and shells were considered and identification methods were reviewed.

Ruotolo et al. [13] investigated the response of a vibrating cantilever beam with a closing crack under sinusoidal loads at various frequencies. In this work, the crack was modelled as fully open or fully closed, while the undamaged part of the beam was modelled by Euler-type finite elements with two nodes and two degrees of freedom at each node. Incremental form for the cracked beam were solved with an implicit time integration, which means that new stiffness matrices were formed at each time step. They illustrated that frequency response functions are strongly depend upon the position of the crack, and this fact may be used for damage detection. In a later work, Ruotolo and Surace [14] developed a method for non-destructive detection and sizing of cracks in beams by using the modal parameters of the lower modes.

Nandwana and Maiti [15] applied the method proposed by Rizos, Asparagathos and Dimaragonas [5] for the detection of location and size of a crack in a stepped cantilever beam based on measurements of the first three natural frequencies. They obtained curves for the variation of stiffness with crack location basing on the measured natural frequencies, and graphed them on the same axes. From the intersection of these curves, the crack location was extracted. The crack size was determined by using the relationship between stiffness and crack size obtained by Ostachowicz and Krawkczuk [7].

Chati et al [16], performed modal analysis of a cantilever beam with a transverse edge crack by modelling the opening and closing of a crack as a piecewise linear system. In this work, a finite element model was used with crack-close and crack-open cases. For each of the linear regions, an eigenvalue problem was defined and then the two sets of natural frequencies were combined to develop the "effective natural frequencies" of the cracked beam. In order to verify the results, a two degree of freedom piecewise-linear system was used and the nonlinear normal modes of vibration were obtained by perturbation methods.

Chondros et al [17] developed a continuous cracked beam vibration theory for longitudinal vibrations of Euler-Bernoulli beams with an edge crack by using Hu-Washizu-Barr variational formulation to develop the differential equation and the boundary conditions of cracked beam.

Boltezar et al [18] presented a procedure to detect a crack site on free-free uniform beams, where a crack is introduced into the system model with an equivalent linear spring connecting two segments of the beam.

Rivola and White [19], studied the effects of crack closure on the dynamic behaviour of the cantilever beams. The system response was analyzed by using bispectral analysis.

Masoud et al. [20] investigated the coupling effect between the crack depth

and the axial load on the natural frequencies of an axially loaded fixed-fixed Euler-Bernoulli beam with symmetrical double sided crack.

Cheng et al. [21] investigated dynamic behaviour of a a cracked cantilever beam modelled as a one degree of freedom lumped parameter system vibrating at its first mode. The stiffness of the structure was modelled as a continuous function having regions corresponding to fully open, partially open and fully closed phases of the crack. The analysis was performed at both time and frequency domains. In this work, it is concluded that the reduction in natural frequency is much more smaller for a continuous breathing crack (or fatigue crack as they called) than an open crack; therefore fatigue cracks would be difficult to be recognized by frequency monitoring and a crack detection procedure by an open crack model would underestimate the "crack severity". It is suggested that detection of fatigue cracks should base on nonlinear features of frequency response functions rather than changes in natural frequencies.

Shifrin and Ruotolo [22] developed a method to calculate the natural frequencies of a beam with multiple open cracks where the cracks are represented as massless rotational springs. But their study was restricted to uniform beams only.

Chinchalkar [23] developed a numerical method to locate the crack in a beam of varying depth with different boundary conditions. Finite element analysis

was used to solve the model where the effect of the crack was taken into account as a rotational spring between two adjacent nodes. For each of three measured natural frequencies, the graphs of stiffness versus crack location were plotted on to same graph and from the intersection of these three curves, the crack locations were extracted.

Khan et al. [24], demonstrated that structural defects can be detected and located using a continously scanning laser Doppler vibrometer.

Lee and Chung [25], presented a method for identifying a crack on a beam type structure by using natural frequency data. They developed a FEA model of the cracked structure by using strain energy concept and modified the system parameters until the first natural frequency of the FE model is equal to the experimental value, from where they identified the crack depth. By utilizing the Gudmunson equation (a relation between the crack size ratio, crack position ratio and undistorted natural frequency), they estimated the location of the crack.

Tysfansky and Bresnevich [26], worked on mathematical simulations of bending vibrations of a cracked aeroplane wing subject to harmonic excitation. They recognized the influence of fatigue crack on the excitation of superharmonic responses within the structure.

Khiem and Lin [27], carried out a natural frequency analysis for a multiple cracked beam on the basis of the transfer matrix method, in which the cracks were modelled as rotational springs. The effects of positions and depths of multiple cracks upon the natural frequencies of the beam were sought. Positions on the beam at which cracks do not affect certain natural frequencies were found, and they are called critical points. In this study, it suggested that this property may be used to detect crack position when it is recognized that a certain frequency is unchanged.

Kerschen and Golinval [28], utilized the restoring force surface method for the identification of a bilinear beam from the measured dynamic response. The beam was modelled as a single degree of freedom system.

Viola et al. [29] developed a crack identification method to locate the crack and to calculate the depth of it by using modal data for a Timoshenko Beam modelled by finite elements. They constructed three dimensional surfaces for the first three natural frequencies based upon the dimensionless crack location and crack depth parameters. They also formed error functions for the mode shapes of the cracked beam.

Krawczuk [30] proposed a method for damage detection in beamlike structures basing on the "genetic algorithm" and gradient-search technique. The beam was modelled with a transverse and non-propagating crack by applying

"spectral beam finite element method" and then an objective error function was formed depending upon the changes in measured dynamic responses of a cracked beam. Then the size and the location of the crack was estimated by an iterative procedure comparing the measured values with the values obtained from calculations for various locations and crack sizes.

Saavedra and Cuitino [31], developed a cracked finite element flexibility matrix, based on strain energy density function given by linear fracture mechanic theory, to be used in finite element analysis of crack systems. A time varying "stiffness matrix" due to the opening and closing of the crack was formulated by using a step function. They studied the dynamic response of a cracked free-free beam and a U-frame excited by a harmonic force. It was found out that noticeable changes occur in the frequency spectra of the steady state vibrations of a damaged beam, such as additional peaks at the harmonics of the forcing frequency especially at even harmonics.

Li [32] developed a method for determining the natural frequencies and mode shapes of a multi-step beam with arbitrary number of cracks. The local flexibility induced by cracks was modelled with massless rotational springs.

Leonard et al. [3] investigated the effects of a crack on modal behaviour of a cantilever beam. They used damping criterion, harmonic distortion criterion, bispectrum transform and auto-bicoherent frequency spectrograms and

coherent power of amplitude modulation tools for the crack detection purposes.

Sinha et al. [33] developed a method to locate and identify the cracks on a beam by using a gradient-based updating technique. Euler-Bernoulli beam elements were used and the effect of the crack to the system was introduced by a variation in the local flexibility parameter EI. The crack was assumed to be always open. In a later work, Sinha and Friswell [34], sought experimental vibration behaviour of a free-free beam with a breathing crack under harmonic excitation. Open-crack and close-crack phases were assumed to be obtained depending on the harmonic forcing applied.

Pugno and Surace [35] introduced a technique to simulate the dynamic response of a beam with several breathing cracks subjected to harmonic excitation. By using harmonic balance method, they obtained a nonlinear system of algebraic equations and solved them iteratively to evaluate the response of a cracked beam.

Kim et al. [36,37] introduced a methodology to locate and estimate the size of damage in structures when a few natural frequencies or a few mode shapes were available. The method used a damage index algorithm that was based on the changes in modal strain energy.

Waldron et al. [38], developed the so called operational deflection curves which are the actual vibration displacement and velocity patterns of a damaged

14

structure that is vibrating at steady-state. They found out that the damage was easier to detect at higher natural modes and also when the excitation point is close to the damaged area.

Apart from identifying cracks in beams, several studies were performed for detecting and identifying any kind of nonlinearity in system. Rice [39] proposed a method to identify weakly nonlinear systems by using equivalent linearization. In this method, the equivalent linear stiffness and damping coefficient values were found out for each response level and a curve was fit to the changing equivalent stiffness and damping values. He tested the method on an aircraft trim panel connector and verified the mathematical model he developed by exciting the system by random forcing. Lin and Ewins [40] developed a technique to localize nonlinearities in stiffness elements using measured data. The method requires response measurements at least two different excitation levels. The method was tested on an actual experimental system as well. The method gives the coordinates that have stiffness type of nonlinear element. Lee and Park [41] proposed a method for identifying nonlinearities in a structure. They found a restoring force vector through the difference of applied external force vector and the inertial force vector. The restoring force vector was used to obtain the linear equivalent of the system for that excitation level by minimizing the sum of squared error of actual and linearized restoring force vectors. Using the linear equivalent stiffness and damping matrices, the error matrix and the error vectors were obtained. Using the error matrix and error vectors, coordinates with nonlinear elements can be

obtained. Crawley and Aubert [42] introduced a force state mapping method for the identification of structural nonlinear elements. Restoring force method was utilized to identify the nonlinearities. The restoring force versus displacement and velocity of the degree of freedom under consideration was plotted as a three-dimensional curve. The smooth linear surface of restoring force indicates that the system is linear. On the other hand, any surface distortion indicates the existance of a nonlinearity either in terms of displacement or velocity.

Recently, Özer and Özgüven [43,44] proposed a technique for localization of nonlinearity in multi-degree of freedom systems by using first order frequency response function data. By this method, localization of the coordinate to which nonlinear elements are connected, and the parametric identification of nonlinearity provided that nonlinearity is present only at ground connection of the structure, can be achieved.

2.2 Present Study

The methods suggested, some of which are mentioned above, for crack detection in structures mainly utilize the shifts in natural frequencies and the changes in mode shapes. Three dimensional surfaces or two dimensional patterns or analytical expressions for the first two or three natural frequencies are constructed or error functions for the mode shapes of the cracked structure are

constructed for the identification purposes, which are based upon the dimensionless crack location and crack depth parameters. Frequency response functions, on the other hand, are used only to detect the damage by searching for the nonlinear features of frequency response functions such as side peaks around the resonant frequencies.

In this thesis, a new method to detect and locate a crack in a structural component is introduced. The method proposed is an extension of a recently developed technique for identification of non-linearity in vibrating multi degree of freedom systems. The method exploits the nonlinear frequency response functions for the detection and identification of cracks in structures.

In Chapter 3, modelling of cracks in beams is presented. The necessary formulations and concepts for the suggested method are given in Chapter 4 and Chapter 5.

Several case studies are examined in Chapter 6. Discussions on the application results are performed in the same chapter.

Finally; conclusions, recommendations and future work are presented in Chapter 7.

CHAPTER 3

MODELLING OF CRACKS IN BEAMS

A crack in a solid can be stressed in three different modes [45], as illustrated in Figures 3.1, 3.2 and 3.3. Normal stresses lead to "opening mode" or mode I. In this mode, displacements of crack surfaces remain perpendicular to the plane of the crack. In "sliding mode" or mode II, in-plane shear occurs. The crack surfaces remain in the same plane of the crack and perpendicular to the leading edge of the crack. In the "tearing mode" or mode III, however, out-of-plane shear occurs where crack surface displacements remain in the plane of the crack and paralel to the leading edge of the crack. For a general loading, the superposition of the three modes is required to describe the behaviour of a cracked beam.
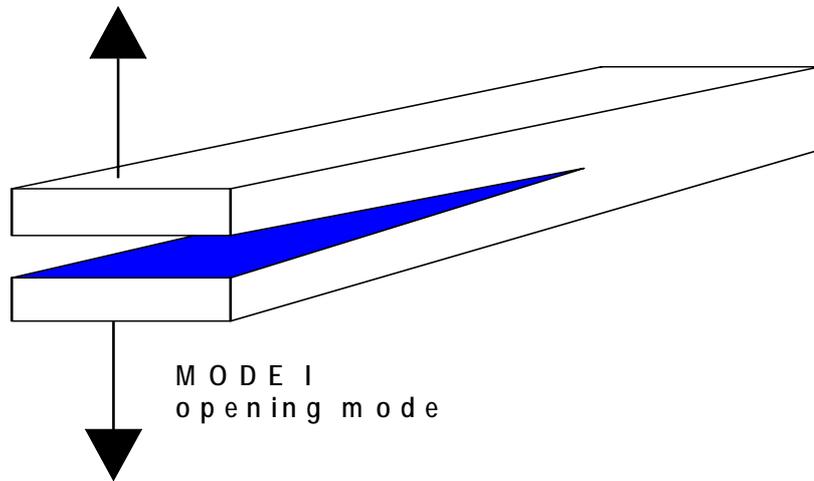
Figure 3.1 Opening mode of crack surfaces
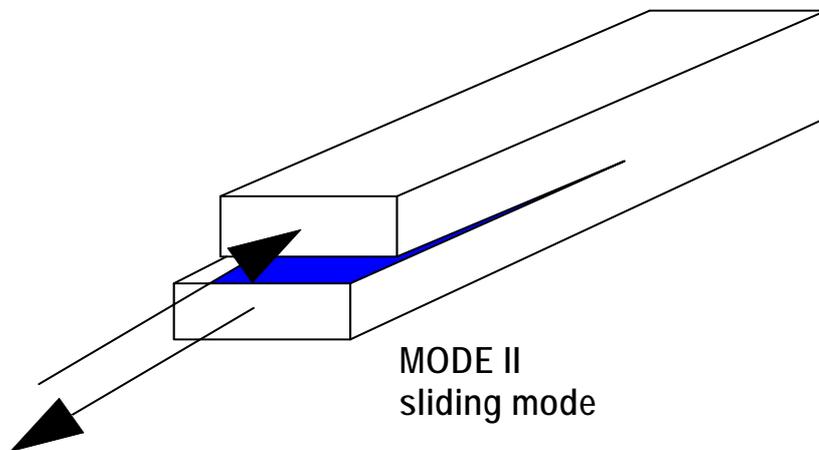
Figure 3.2 Sliding mode of crack surfaces

MODE III
tearing mode
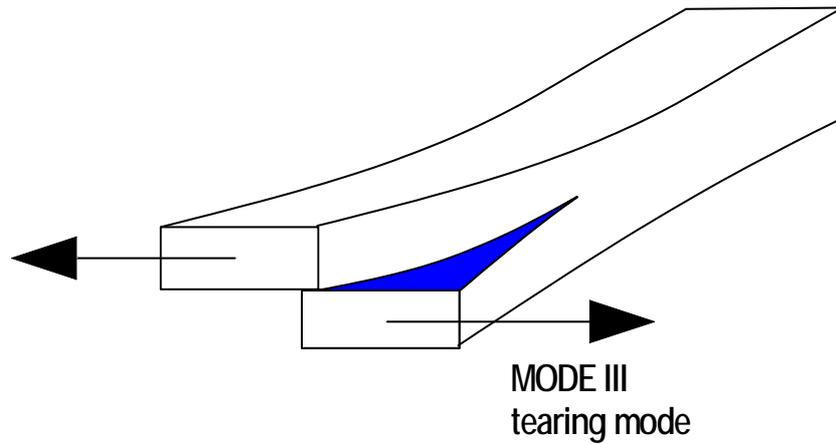
Figure 3.3 Tearing mode of crack surfaces

A crack on a structural member induces a local flexibility which is a function of the crack depth. It can be included into the system by an additional strain energy. This energy of the crack yields a local flexibility coefficient, which can be expressed by stress intensity factors calculated by means of the Castigliano's theorem in the linear elastic range [46].

Figure 3.4 shows a prismatic beam under general loading, with a crack depth a along the z axis. The beam is excited by an axial force P_1, shear forces P_2, P_3, and bending moments P_4 and P_5.
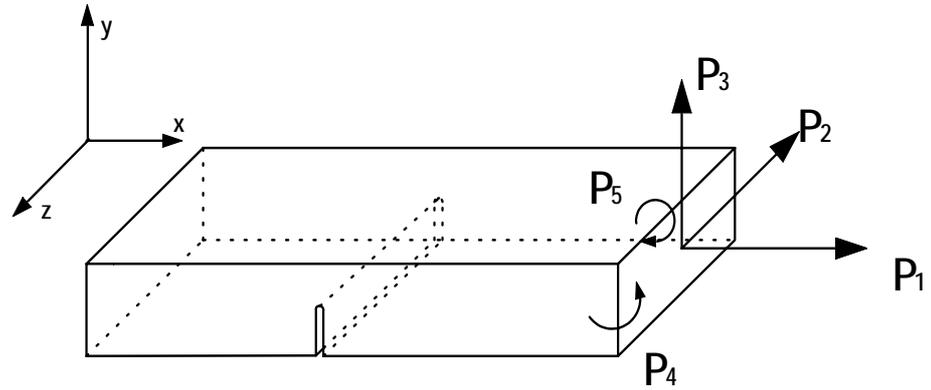
Figure 3.4   Beam element with transverse crack under general loading

The Castigliano's Theorem states that *the partial derivative of the strain energy of a structure with respect to any load is equal to the displacement corresponding to that load* [47]. Therefore, the additional displacement δ_i along the direction of force P_i due to the presence of a crack may be calculated by using Castigliano's theorem as follows:

$$\delta_i = \frac{\partial W^{(1)}}{\partial P_i} \tag{3.1}$$

where $W^{(1)}$ denotes the additional strain energy due the presence of a crack, and can be expressed as [46],

$$W^1 = \int_0^a (\frac{\partial W^1}{\partial a})da = \int_0^a Jda \qquad (3.2)$$

where $J = \partial W^1/\partial a$ is the strain energy density function. Therefore, Equation 3.1 can be written as

$$\delta_i = \frac{\partial}{\partial P_i}\left[\int_0^a J(a)da\right] \qquad (3.3)$$

Since Castigliano's theorem provides a mean for finding deflections of structure by using the strain energy of the structure, the second derivative of the strain energy with respect to the load leads to the flexibility influence coefficients such as

$$c_{ij}^{(1)} = \frac{\partial \delta_i}{\partial P_j} = \frac{\partial^2 W^{(1)}}{\partial P_i \partial P_j} = \frac{\partial^2}{\partial P_i \partial P_j}\int_0^a J(a)da \qquad (3.4)$$

The strain energy density function J, in Equation 3.4, has the following form [46,48]

$$J = \frac{b}{E'}\left[(\sum_{n=1}^{5} K_{In})^2 + (\sum_{n=1}^{5} K_{IIn})^2 + (1+v)(\sum_{n=1}^{5} K_{IIIn})^2\right] \qquad (3.5)$$

22

where $E'=E$ for plane stress assumption, $E'=E/(1-\nu^2)$ for plane strain assumption, E is the elastic modulus and ν is the Poisson's ratio, K_I, K_{II}, K_{III} are stres intensity factors for opening type, sliding type and tearing type cracks, respectively. Here n denotes the loading type and takes values 1 to 5 (See Figure 3.4). Substituting Equation 3.5 into Equation 3.4 yields

$$c_{ij}^{(1)} = \frac{1}{E'b} \int_0^a \left[\frac{\partial^2}{\partial P_i \partial P_j} \sum_m (\kappa_m \sum_n K_{mn})^2 \right] da \qquad (3.6)$$

where $\kappa_m = (1+\nu)$ for m=III and $\kappa_m = 1$ for m=I, II and K_{mn} is the stress intensity factor of mode m (m=I, II, III) due to the forcing P_n (n=1, 2, 3, 4, 5).

Equation 3.6 gives the flexibility coefficients for general loading. For simplicity, by neglecting axial loads P_1 and P_2 and the moment P_4 about y axis, considering only $P=P_3$ and $M=P_5$, from Equations 3.2 and and 3.5, the following expression can be obtained for the additional strain energy

$$W^1 = b \int_0^a ((K_{IM} + K_{IP})^2 + K_{IIP}^2)/E')da, \qquad (3.7)$$

where [46]

$$K_{IM} = (6M/bh^2)\sqrt{\pi a}F_I(s), \tag{3.8}$$

$$K_{IP} = (3PL/bh^2)\sqrt{\pi a}F_I(s), \tag{3.9}$$

$$K_{IIP} = (P/bh)\sqrt{\pi a}F_{II}(s), \tag{3.10}$$

$$F_I(s) = \sqrt{(2/\pi s)\tan(\pi s/2)}\,\frac{0.923 + 0.199(1 - \sin(\pi s/2))^4}{\cos(\pi s/2)} \tag{3.11}$$

$$F_{II}(s) = (3s - 2s^2)\frac{1.122 - 0.561s + 0.085s^2 + 0.18s^3}{\sqrt{1-s}} \tag{3.12}$$

Having the analytical expression for W^1, the additional flexibility coefficient may be calculated as

$$c_{ij}^{(1)} = \frac{\partial^2 W^{(1)}}{\partial P_i \partial P_j}, \qquad P_1 = P, \quad P_2 = M, \quad i,j = 1,2. \tag{3.13}$$

The strain energy of a finite beam element without a crack, on the other hand, can be written by neglecting shear force, as

$$W^0 = \frac{1}{2EI} \int_0^L (M+P)dz \qquad (3.14)$$

$$W^0 = \frac{P^2 L^3}{6EI} + \frac{PML^2}{2EI} + \frac{M^2 L^3}{2EI} \qquad (3.15)$$

From Equation 3.13, the flexibility coefficient for the uncracked case can also be obtained as

$$c_{ij}^{(0)} = \frac{\partial^2 W^{(0)}}{\partial P_i \partial P_j}, \qquad P_1 = P, \qquad P_2 = M, \qquad i,j = 1,2, \qquad (3.16)$$

Then the total flexibility coefficient becomes

$$c_{ij} = c_{ij}^{(0)} + c_{ij}^{(1)}. \qquad (3.17)$$

By using the equilibrium condition, (See Figure 3.5)

$$(P_i \quad M_i \quad P_{i+1} \quad M_{i+1})^T = [T](P_{i+1} \quad M_{i+1})^T, \qquad (3.18)$$

where

$$[T] = \begin{bmatrix} -1 & -L & 1 & 0 \\ 0 & -1 & 0 & 1 \end{bmatrix}^T \qquad (3.19)$$

and using the principle of virtual work, the stiffness matrix of the undamaged finite element can be written as;

$$\left[K \right]_{ue} = \left[T \right]^{T} \left[c^{(0)} \right]^{-1} \left[T \right]. \tag{3.20}$$

$$\left[K \right]_{ue} = \frac{EI}{L^{3}} \begin{bmatrix} 12 & 6L & -12 & 6L \\ 6L & 4L^{2} & -6L & 2L^{2} \\ -12 & -6L & 12 & -6L \\ 6L & 2L^{2} & -6L & 4L^{2} \end{bmatrix}, \tag{3.21}$$

and for the cracked finite element;

$$\left[K \right]_{ce} = \left[T \right]^{T} \left[c^{(1)} \right]^{-1} \left[T \right]. \tag{3.22}$$

$$\left[K \right]_{ce} = \left[T \right]^{T} \begin{bmatrix} \dfrac{\partial^{2} W^{(1)}}{\partial P \partial P} & \dfrac{\partial^{2} W^{(1)}}{\partial P \partial M} \\ \dfrac{\partial^{2} W^{(1)}}{\partial M \partial P} & \dfrac{\partial^{2} W^{(1)}}{\partial M \partial M} \end{bmatrix}^{-1} \left[T \right]. \tag{3.23}$$
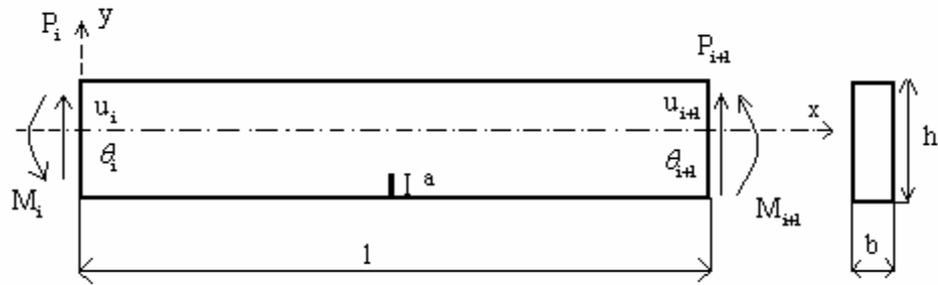
Figure 3.5 Beam finite element.

According to the Saint-Venant principle, the stress field in a structure with a crack is affected only in the region adjacent to the crack. This means that the finite element stiffness matrix of an uncracked element adjacent to an element with crack may be regarded as unchanged. Therefore, while constructing the global stiffness matrix of the structure when the nonlinearity caused by the crack is excited, changing or updating only the cracked finite beam element matrix would be valid.

It is assumed that the presence of the crack does not affect the mass $[M]$ and the damping $[C]$ matrices. For a single FE , the mass matrix may be formulated as follows [49],

$$[M]_e = \frac{\rho AL}{420} \begin{bmatrix} 156 & 22L & 54 & -13L \\ 22L & 4L^2 & 13L & -3L^2 \\ 54 & 13L & 156 & -22L \\ -13L & -3L^3 & -22L & 4L^2 \end{bmatrix} \qquad (3.24)$$

where ρ is the density of the beam material and A is the cross sectional area of the finite beam element.

If modal damping is assumed, then the damping matrix can be defined as

$$[C]_e = (\Xi^T)^{-1} \Pi \Xi^{-1} \qquad (3.25)$$

where Ξ is the mass normalized modal matrix and Π is

$$[\Pi] = 2 \begin{bmatrix} \zeta_1 \omega_{n1} & 0 & . & . & 0 \\ 0 & \zeta_2 \omega_{n2} & . & . & 0 \\ . & . & . & . & . \\ . & . & . & . & . \\ 0 & 0 & . & . & \zeta_n \omega_{nn} \end{bmatrix} \qquad (3.26)$$

Here, ζ_i is the ith modal damping ratio and ω_{ni} is the ith natural frequency.

CHAPTER 4

QUASILINEARIZATION OF NONLINEAR MULTI DEGREE OF FREEDOM SYSTEMS

4.1 Introduction

A linear system is the one whose performance obeys the principle of superposition. The principle of superposition states that if an input $f_1(t)$ produces the output $x_1(t)$ and an input $f_2(t)$ produces the output $x_2(t)$, then for the input $af_1(t) + bf_2(t)$, where a and b are constants, the response will be $ax_1(t) + bx_2(t)$, for all $f_1(t)$, $f_2(t)$, a and b. A nonlinear system, on the other hand, may be defined as the one for which the principle of superposition is not valid, which means that, the response of the system to an input can not be found although the response to some other input is known.

If a linear structure is excited harmonically then its steady state response will be harmonic with a frequency equal to the excitation frequency and frequency response function will be independent of force amplitude. Steady state response of a nonlinear structure excited by harmonic forcing, on the other hand, may consist of subharmonics, a bias term, fundamental harmonic, and superharmonics. Therefore, the frequency response characteristics will become extremely sensitive to the input type, amplitude, frequency and initial conditions that the system is exposed to.

4.2 Describing Functions

To deal with nonlinear problems, an approximate analysis called quasi-linearization is widely utilized [50-53]. The term Quasi-linearization is used for simply replacing the system nonlinearity by an approximate linear gain which depends upon the type, amplitude and the frequencies of the input. These linear gains, or the quasi-linear approximating functions, are commonly called as Describing Functions (DF). The basic idea is to design a linear approximator to minimize the mean-squared difference between the output of that approximator and the output of the nonlinearity [54].

The describing function method is closely related to the method of slowly varying amplitude and phase, which is proposed by Krylov and Bogoliubov [55] and Bogoliubov and Mitropolsky [54].

The describing function linearises the nonlinearity by defining a transfer function as the relation of the fundamental components of the input and output. Consider a nonlinearity

$$n(y, \dot{y}) \qquad (4.1)$$

which is excited by a sinusoidal input in the form

$$y = Y \sin(\psi), \qquad (4.2)$$

where $\psi = \omega t$ and dot denotes differentation with respect to time. The nonlinearity for this input can be expressed by using Fourier series expansion as

$$n(Y \sin(\psi), \omega Y \cos(\psi)) = \sum_{m=1}^{\infty} A_m(Y, \omega) \sin(m\omega t + \varphi_m(Y, \omega)), \qquad (4.3)$$

Describing function v can be defined as

$$v(Y, m\omega) = \frac{\text{phasor representation of ouput component at frequency } m\omega}{\text{phasor representation of input component at frequency } m\omega} \qquad (4.4)$$

$$= \frac{A_m(Y, \omega)}{Y} e^{i\varphi_m(Y, m\omega)} \qquad (4.5)$$

Describing function approach assumes that the linear part of the system acts as a very good low-pass filter [56]. This means that, generally, the higher harmonics of the output are excluded in the describing function formulation, and only the fundamental harmonic component is taken into consideration. (Figure 4.1)

$$n_1(Y,\omega) = A_1 \sin(\omega t + \varphi_1)$$

$$n_r(Y,\omega) = \sum_{m=2}^{\infty} A_m \sin(m\omega t + \varphi_m)$$
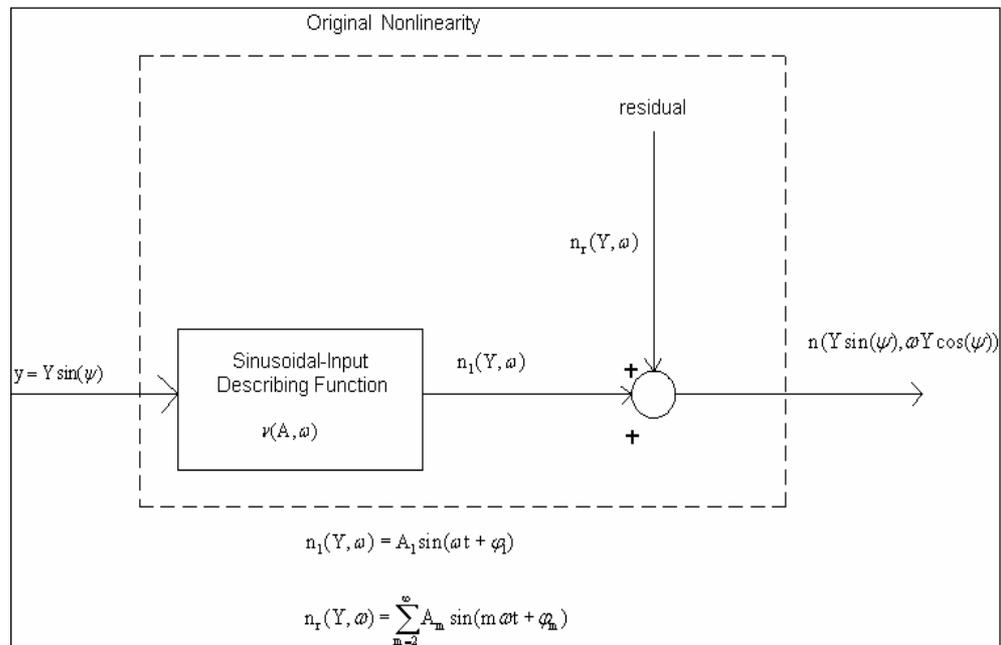
Figure 4.1 Definition of describing function

The describing function for $n(y,\dot{y})$, therefore, can be found by multiplying both sides of equations by $\sin(\psi)$ and $\cos(\psi)$, and then integrating with respect to ψ :

32

$$A_1 \cos(\psi) = \frac{1}{\pi} \int_0^{2\pi} n(Y\sin(\psi), Y\omega\cos(\psi))\sin(\psi)\,d\psi, \qquad (4.6)$$

$$A_1 \sin(\psi) = \frac{1}{\pi} \int_0^{2\pi} n(A\sin(\psi), A\omega\cos(\psi))\cos(\psi)\,d\psi, \qquad (4.7)$$

Multiplying Equation (4.6) by i and adding to Equation (4.7), and then dividing both sides of the resultant equation by Y yield the most general form of the sinusoidal-input describing function:

$$\nu(A, \omega) = \frac{A_1}{Y} e^{i\varphi_1} = \frac{i}{\pi A} \int_0^{2\pi} n(Y\sin(\psi), Y\omega\cos(\psi)) e^{-i\psi}\,d\psi \qquad (4.8)$$

In order to explain the use of describing functions in calculating harmonic response of nonlinear systems, consider a SDOF system with a nonlinear restoring force excited by a harmonic force:

$$m\ddot{x} + C\dot{x} + Kx + n(x, \dot{x}) = F\sin(\omega t). \qquad (4.9)$$

In order to solve this problem by describing function method, the response of the nonlinear system x(t) is assumed to be close enough to a sinusoidal oscillation as:

$$x \cong \overline{X} \sin(\omega t + \gamma) = \overline{X} \sin(\psi) \qquad (4.10)$$

where $\overline{X}$ is the response amplitude, ω is the excitation frequency, and γ is the phase angle.

Since the variable x(t) is assumed to have a sinusoidal form, then the nonlinear function $n(x, \dot{x})$ may be complex and will be a periodic function of time. Therefore, it can be expressed in a Fourier series as:

$$n(x, \dot{x}) = N_0(\omega, \overline{X}) + N_1(\omega, \overline{X}) \overline{X} \sin(\omega t + \gamma)$$
$$+ iN_2(\omega, \overline{X}) \overline{X} \sin(\omega t + \gamma) + HigherOrderTerms. \qquad (4.11)$$

where the bias term is

$$N_0 = \frac{1}{2\pi} \int_0^{2\pi} N(\overline{X} \sin(\psi), \omega \overline{X} \cos(\psi)) d\psi, \qquad (4.12)$$

and the real and the imaginary parts of the fundamental harmonic are

$$N_1 = \frac{1}{\pi \overline{X}} \int_0^{2\pi} N(\overline{X}\sin(\psi), \omega\overline{X}\cos(\psi))\sin(\psi)\mathrm{d}\psi, \tag{4.13}$$

$$N_2 = \frac{1}{\pi \overline{X}} \int_0^{2\pi} N(\overline{X}\sin(\psi), \omega\overline{X}\cos(\psi))\cos(\psi)\mathrm{d}\psi. \tag{4.14}$$

The Equation given by (4.11) can be defined as the optimum equivalent linear complex stiffness representation of the nonlinear function $n(x, \dot{x})$ when the response of the nonlinear system x(t) is close enough to a sinusoidal oscillation. If $n(x, \dot{x})$ is symmetrical around the origin, then N_0 becomes zero. If the nonlinearity is not frequency dependent, then N_2 becomes zero.

4.3 Response Analysis of Nonlinear Structures due Periodic Excitation

Consider a nonlinear structure, vibrating under the effect of a periodic external forcing. If the structure is modelled as a discrete system with n degrees of freedom, then the matrix differential equation of motion can be written as

$$[M]\{\ddot{x}\} + [C]\{\dot{x}\} + [K]\{x\} + \{N\} = \{f\}, \tag{4.15}$$

where [M], [C], [H] and [K] denote linear mass, viscous damping, structural damping and stiffness matrices, respectively. $\{x\}$ is the vector of generalized displacements. $\{f\}$ and $\{N\}$ denote the external forcing and the internal nonlinear forces, respectively.

The kth element of $\{N\}$ can be defined as a sum

$$N_k = \sum_{j=1}^{n} n_{kj}, \tag{4.16}$$

where n_{kj} denotes the nonlinear restoring force element acting between the coordinates k and j when $k \neq j$, and between the ground and the coordinate k when $k = j$. n_{kj} may be a function of inter-coordinate displacements and their derivates such that

$$n_{kj} = n_{kj}(y_{kj}, \dot{y}_{kj}, \ddot{y}_{kj}, \dot{y}_{kj,...}), \tag{4.17}$$

where

$$y_{kj} = x_k - x_j, \text{ when } k \neq j, \tag{4.18}$$

$$y_{kj} = x_k, \text{ when } k = j. \tag{4.19}$$

and has the following symmetry property:

$$n_{kj} = n_{jk}. \tag{4.20}$$

The external periodic forcing can be represented as a sum of infinite number of sinusoids such as:

$$\{f\} = \sum_{m=0}^{\infty} \{f\}_m = \text{Im}(\sum_{m=0}^{\infty} \{F\}_m e^{im\psi}), \tag{4.21}$$

where

$$\psi = \omega t. \tag{4.22}$$

$\{F\}_m$ is the real vector corresponding to the forcing amplitude of the mth harmonic. The response of the structure due to this periodic excitation can be defined as

$$\{x\} = \sum_{m=0}^{\infty} \{x\}_m = \text{Im}(\sum_{m=0}^{\infty} \{X\}_m e^{im\psi}). \tag{4.23}$$

The kth element of the complex vector $\{X\}_m$ can be written as

$$\left(X_k \right)_m = (\overline{X_k})_m \, e^{i(\vartheta_k)_m}. \tag{4.24}$$

$(\overline{X_k})_m$ and $(\vartheta_k)_m$ are the real displacement amplitude and the phase for the kth coodinate and for the harmonic component with the frequency $m\omega$. Note that

$$\{X\}_0 = \{\overline{X}\}_0. \tag{4.25}$$

Similar to Equations (4.23), (4.24) and (4.25), the inter-coordinate relative displacements and nonlinear restoring force elements can be represented as:

$$y_{kj} = \sum_{m=0}^{\infty} (y_{kj})_m = \mathrm{Im}(\sum_{m=0}^{\infty} (Y_{kj})_m e^{im\psi}), \tag{4.26}$$

where

$$(Y_{kj})_m = (X_k)_m - (X_j)_m, \quad \text{when} \quad k \neq j, \tag{4.27}$$

and

$$(Y_{kk})_m = (X_k)_m, \tag{4.28}$$

As in Equation (4.25), $(Y_{kj})_m$ may be expressed as,

$$(Y_{kj})_m = (\overline{Y_{kj}})_m e^{i(\beta_{kj})_m}, \tag{4.29}$$

and

$$(Y_{kj})_0 = (\overline{Y_{kj}})_0, \tag{4.30}$$

For the nonlinear restoring force element,

$$n_{kj} = \sum_{m=0}^{\infty} (n_{kj})_m = \text{Im}(\sum_{m=0}^{\infty} (A_{kj})_m e^{im\psi}), \tag{4.31}$$

$$(A_{kj})_m = (\overline{A_{kj}})_m e^{i(\phi_{kj})_m}, \tag{4.32}$$

$$(A_{kj})_0 = (\overline{A_{kj}})_0. \tag{4.33}$$

The series expression for n_{kj} consists of the bias term with real amplitude $(\overline{A_{kj}})_0$ and sinusoidal terms with complex amplitudes $(A_{kj})_m$. $(\overline{A_{kj}})_0$ and $(A_{kj})_m$ can be found out by using the Fourier integrals given below:

$$(\overline{A_{kj}})_0 = \frac{1}{2\pi} \int_0^{2\pi} n_{kj} d\psi \tag{4.34}$$

$$(A_{kj})_m = \frac{i}{\pi} \int_0^{2\pi} n_{kj} e^{-im\psi} d\psi, \quad m \geq 1. \tag{4.35}$$

In evaluating the above integrals, the following form of y_{kj} is used:

$$y_{kj} = \sum_0^{\infty} (\overline{Y_{kj}})_m \sin(m\psi + (\beta_{kj})_m). \tag{4.36}$$

The describing function of order m, $(\nu_{kj})_m$, can be defined as the optimum equivalent quasi-linear complex gain of the nonlinear force n_{kj} for the harmonic displacement $(y_{kj})_m$, and can be expressed as

$$(\nu_{kj})_m = \frac{(A_{kj})_m}{(Y_{kj})_m}. \tag{4.37}$$

$(v_{kj})_m$ can be found by using the following integrals:

$$(v_{kj})_0 = \frac{1}{2\pi(\overline{Y_{kj}})_0} \int_0^{2\pi} n_{kj} \, d\psi, \qquad\qquad (4.38)$$

$$(v_{kj})_m = \frac{i}{\pi(Y_{kj})_m} \int_0^{2\pi} n_{kj} e^{-im\psi} \, d\psi, \quad m \geq 1, \qquad\qquad (4.39)$$

$$(v_{kj})_m = (v_{kj})_m \, (\omega, (Y_{kj})_m), \qquad m = 0,1,2,3,4,..... \qquad\qquad (4.40)$$

The internal nonlinear forces can be expressed in terms of the describing functions as:

$$n_{kj} = \mathrm{Im}(\sum_{m=0}^{\infty} (v_{kj})_m (Y_{kj})_m e^{im\psi}), \qquad\qquad (4.41)$$

$$\{N\} = \sum_{m=0}^{\infty} \{n\}_m = \mathrm{Im}(\sum_{m=0}^{\infty} \{\mathbb{N}\}_m e^{im\psi}). \qquad\qquad (4.42)$$

$\{\mathbb{N}\}_{\mathrm{m}}$ is the complex amplitude vector of internal nonlinear forces at frequency $\mathrm{m}\omega$. Its kth element is given by:

$$(\mathbb{N}_{\mathrm{k}})_{\mathrm{m}} = \sum_{\mathrm{j}=1}^{\mathrm{n}} (\nu_{\mathrm{kj}})_{\mathrm{m}} (\mathrm{Y}_{\mathrm{kj}})_{\mathrm{m}} \tag{4.43}$$

If Equations (4.21), (4.23) and (4.42) are substituted, in complex form, into the matrix differential Equation of motion (4.15), the following equation can be obtained by grouping terms with same frequencies:

$$[\alpha]^{-1}_{\mathrm{m}} \{\mathrm{X}\}_{\mathrm{m}} + \mathrm{N}_{\mathrm{m}} = \{\mathrm{F}\}_{\mathrm{m}}, \quad (\mathrm{m} = 0,1,2,3,4.....), \tag{4.44}$$

where

$$[\alpha]_{\mathrm{m}} = ([\mathrm{K}] - (\mathrm{m}\omega^2 [\mathrm{M}] + \mathrm{i}\omega[\mathrm{C}] + \mathrm{i}[\mathrm{H}])^{-1}, \tag{4.45}$$

is the receptance matrix of the linear part of the structure at frequency $\mathrm{m}\omega$.

If we express the complex amplitude vector of internal nonlinear force $(\mathbb{N})_m$, as a matrix ($[\Delta]_m$) multipled by the displacement amplitude vector for the mth harmonic, $\{X\}_m$,

$$\{\mathbb{N}\}_m = [\Delta]_m \{X\}_m, \tag{4.46}$$

then from the following equation

$$\{\mathbb{N}_k\}_m = \sum_{j=1}^{n} (\nu_{kj})(Y_{kj})_m = \sum_{j=1}^{n} (\Delta_{kj})(X_{kj})_m, \tag{4.47}$$

we can define the elements of $[\Delta]_m$ as

$$(\Delta_{kk})_m = \sum_{j=1}^{n} (\nu_{kj})_m, \tag{4.48}$$

$$(\Delta_{kj})_m = -(\nu_{kj})_m, \quad k \neq j, \tag{4.49}$$

Inserting Equation (4.46) into Equation (4.44), it can be easily obtained that,

$$\{X\}_m = [\Theta]_m \{F\}_m, \quad (m = 0, 1, 2, 3, 4, \ldots), \tag{4.50}$$

where $[\Theta]_m$ is the response level dependent quasi-linear receptance matrix of the structure at frequency $m\omega$, and can be expressed as,

$$[\Theta]_m = ([K] - (m\omega^2 [M] + i\omega [C] + i[H] + [\Delta]_m). \qquad (4.51)$$

If structure is linear then Equation (4.52) reduces to

$$\{X\}_m = [\alpha]_m \{F\}_m, \quad (m = 0, 1, 2, 3, 4, ...), \qquad (4.52)$$

The linear receptance matrix $[\alpha]_m$ is a function of frequency ω, and linear coefficient matrices of the structure. The pseudo-receptance matrix $[\Theta]_m$, on the other hand, is a function of frequency ω, linear and nonlinear matrices of the structure and all harmonic response amplitudes. Note that, $[\Theta]_m$ is a displacement dependent matrix. Therefore, the response of a nonlinear system can be obtained through Equations (4.51) and (4.50) only by using an iterative procedure.

CHAPTER 5

DETECTION AND LOCALIZATION OF CRACKS IN BEAMS

5.1 Introduction

From Equations (4.51), $[\Delta]_m$ can be obtained as;

$$[\Delta] = [\Theta]^{-1} - [\alpha]^{-1} \tag{5.1}$$

Here and in the following equations, subscript m is dropped for convenience.

Post multiplying both sides of the Equation (5.1) by $[\Theta]$ yields

$$[\Delta][\Theta] = [I] - [Z][\Theta] \tag{5.2}$$

where $[Z]$ is the dynamic stiffness matrix of the linear part of the system, and defined as:

$$[Z] = [\alpha]^{-1} = \left([K] - \omega^2 [M] + i\omega [C] + i[H]\right) \qquad (5.3)$$

The ith column of Equation (5.2) can be expressed as

$$[\Delta]\{\Theta^i\} = \{\varsigma^i\} - [Z]\{\Theta^i\} \qquad (5.4)$$

where $\{\varsigma^i\}$ is a vector of which ith element is unity while all other elements are zero, and $\{\Theta^i\}$ is the ith column of $[\Theta]$. The rth row of Equation (5.4) yields,

$$[\Delta_r]\{\Theta^i\} = \delta_{ir} - [Z_r]\{\Theta^i\} \qquad (5.5)$$

where δ_{ir} is the Kronecker Delta Function, $[\Delta_r]$ and $[Z_r]$ represent the rth rows of $[\Delta]$ and $[Z]$, respectively.

The term $\delta_{ir} - [Z_r]\{\Theta^i\}$, which is defined as "nonlinearity number" NLN$_r$ [41], or may be called as "nonlinearity coefficient" for the rth coordinate, is an indication of nonlinear element connected to coordinate r. This term becomes zero,

if the rth row and column of $[\Delta]$ are all zero. If there is a nonzero element in the rth row or column of $[\Delta]$, then the term $\delta_{ir} - [Z_r]\{\Theta^i\}$ will yield a nonzero value for the rth coordinate, implying that one of the elements that are connected to the rth coordinate is nonlinear. From Equation (5.5), NLN_r can be written as,

$$NLN_r = \Delta_{r1}\Theta_{1i} + \Delta_{r2}\Theta_{2i} + \ldots\ldots + \Delta_{rn}\Theta_{ni} \tag{5.7}$$

or can be written as ,

$$NLN_r = \delta_{ir} - Z_{r1}\Theta_{1i} - Z_{r2}\Theta_{2i}\ldots\ldots - Z_{rn}\Theta_{ni} \tag{5.9}$$

NLN_r can be calculated from the harmonic response of the structure measured at all coordinates connected to the rth coordinate, when the structure is excited at the coordinate i. Here Z is obtained from the response at the low excitation levels, in order to make the structure behave as linear and to get the linear receptance, and Θ is obtained from the response at high excitation levels.

The method described above will be used to detect and locate the cracks which create nonlinearity.

5.2   Computations of the Time Response of a Cracked Beam

In the verification of the crack identification method suggested in this study, instead of experimental study, computer simulation results are used. In order to simulate the dynamic behaviour of a beam with crack, the following method is used. Note that the harmonic balance method given in Chapter 4 could have been used in determining the harmonic response of a nonlinear beam. However, since the identification method is based on the harmonic balance method given in Chapter 4, here a different method is employed for determining the nonlinear time response of the system.

Let us consider the equation of motion for a linear system. After constructing the global mass, stiffness and damping matrices, the governing equation of motion can be written as:

$$[M]\{\ddot{x}\} + [C]\{\dot{x}\} + [K]\{x\} = \{Q\}\sin(\omega t) \qquad (5.10)$$

where

$$\{x\} = (u_1 \quad \theta_1 \quad u_2 \quad \theta_1 \quad .. \quad .. \quad u_n \quad \theta_n)^T ,$$
$$\{Q\} = (Q_1 \quad Q_2 \quad .. \quad Q_n)^T , \qquad (5.11)$$

and u_i, θ_i and Q_i denote the displacement, rotation and external forcing at the ith node, respectively. When Equation (5.10) is represented in state space form, it becomes,

$$\{\dot{q}\} = [A]\{q\} + [B]u \tag{5.12}$$

where

$$\{q\} = \left\{ \begin{array}{c} \{x\} \\ \{\dot{x}\} \end{array} \right\}, \tag{5.13}$$

$$[A] = \begin{bmatrix} [0] & [I] \\ -[M]^{-1}[K] & -[M]^{-1}[C] \end{bmatrix}, \tag{5.14}$$

$$[B] = \left\{ \begin{array}{c} \{0\} \\ [M]^{-1}\{Q\} \end{array} \right\}, \tag{5.15}$$

$$[C] = \begin{bmatrix} [I] & [0] \end{bmatrix}, \tag{5.16}$$

$$u = \sin(\omega t) ,\qquad\qquad\qquad (5.17)$$

$$\{D\} = \{0\} .\qquad\qquad\qquad (5.18)$$

Solutions to Equation (5.12) are obtained by using the integrators in MATLAB R13 ®. Integrations are performed in Simulink for [0~4] or [0~6] seconds for the steady state solutions, using Ode23 (Bogachi-Shampine) and Ode45 (Dormand-Prince) for variable time step, and Ode5 (Dormand-Prince) and Ode4 (Runga-Kutta) for a fixed time step of 0.0001 seconds. For the piecewise stiffness nonlinearity caused by the cracked, the undamaged finite element stiffness matrix $[K]_e$, and the cracked finite element stiffness matrix $[K]_{ce}$, are switched between and updated on the global stiffness matrix for the cracked finite element with the condition upon its rotational coordinates.

Figure 5.1 demonstrates the bilinear stiffness property of a cracked beam. Here m_2 is the stiffness value (corresponding to any rotational or translational coordinate) of an uncracked finite beam element and m_1 is the stiffness value of the uncracked part of a cracked finite beam element. Obviously, m_1 and m_2 take different values for rotational and translational coordinates. Stiffness matrix of an uncracked beam, $[K]_{ue}$, is determined by m_2 values whereas the stiffness matrix for the uncracked part of a cracked beam, $[K]_{ce}$, is determined by m_1 values. Note

that, $[K]_{ce}$ gives the stiffness matrix of a cracked beam element when the crack is open and $[K]_{ue}$ gives the stiffness matrix of the same cracked beam element when the crack is closed. Therefore during a cyclic motion of a cracked beam, at each time step it should be checked whether the crack is open or closed, and the stiffness matrix of the element is to be determined accordingly.
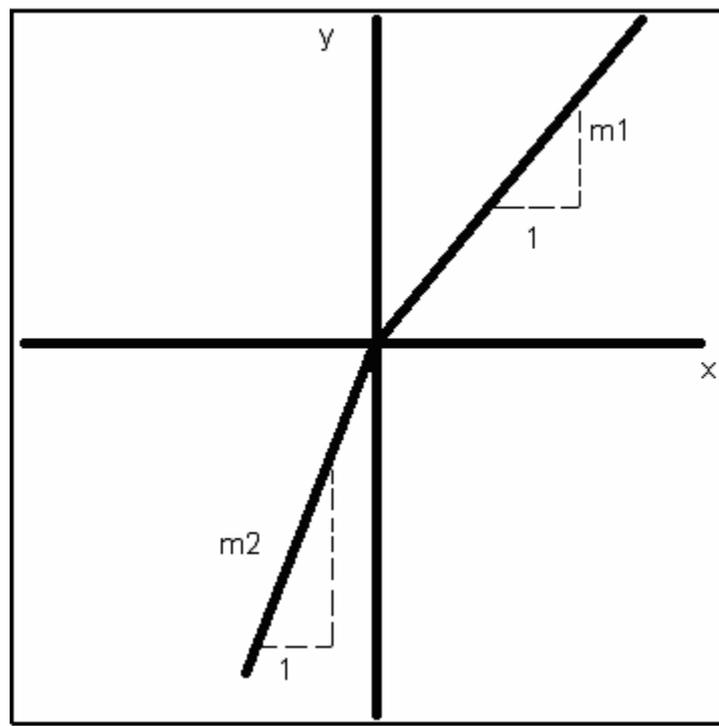
Figure 5.1 Bilinear stiffness model

As it is mentioned in Chapter 1, the roughness of the fracture surface, corrosion debris in the crack, plastic deformation left in the wake of a propagating

crack, strain induced phase transformation in the fatigue zone and hydraulic wedging produced by oil trapped in the crack may lead to partial crack closure [30]. Figure 5.2 demonstrates a typical stiffness curve as a function of the applied load for a cracked beam. Because of the above mentioned interactions between the crack faces, a cracked beam may behave as an uncracked beam until the applied excitation becomes sufficiently high to overcome the closure load. This effect can be included into the crack model in Figure 5.2 by δ.
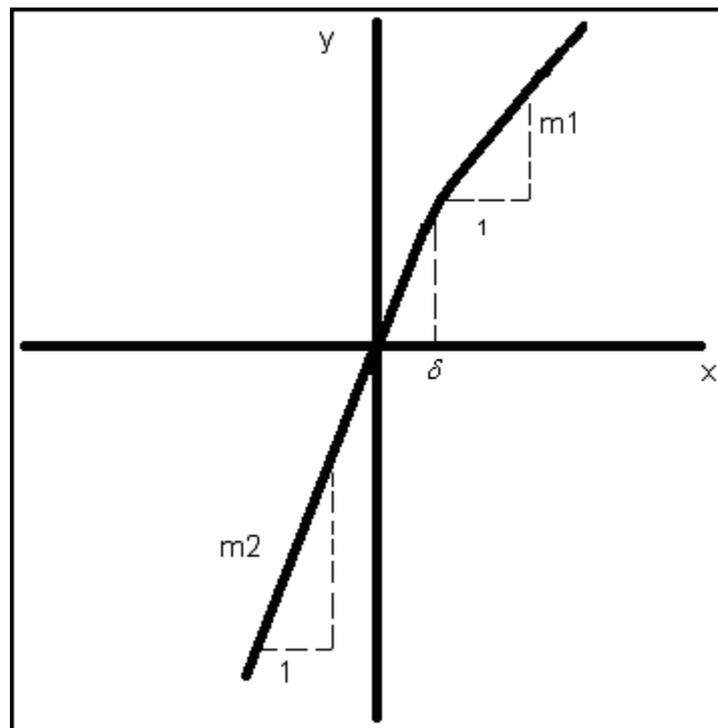
Figure 5.2 Bilinear crack model with crack closure effect

When the crack is located in the lower side of the beam (Figure 5.3), if $\Theta_2 - \Theta_1 < \delta$ then the crack is not open, therefore the nonlinearity is not excited. In this case, undamaged beam finite element stiffness matrix $[K]_e$ is valid on the global stiffness matrix during the simulation. However, when $\Theta_2 - \Theta_1 > \delta$, then the crack is open, so that the nonlinearity is excited. This time, cracked finite element stiffness matrix $[K]_{ce}$ becomes valid on the global stiffness matrix during the simulation. When the crack is located on the upper side of the beam, on the other hand, all conditions upon the rotational coordinates become vice versa, as it can be observed from Figure 5.4.
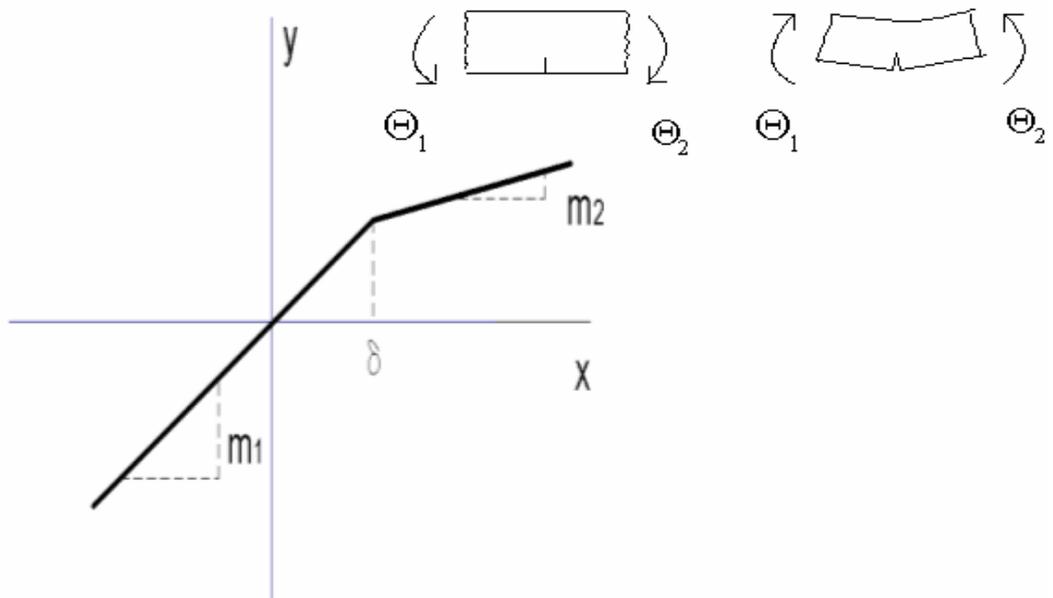
Figure 5.3 Bilinear crack model with crack closure effect,

crack is on the lower side of the beam

53
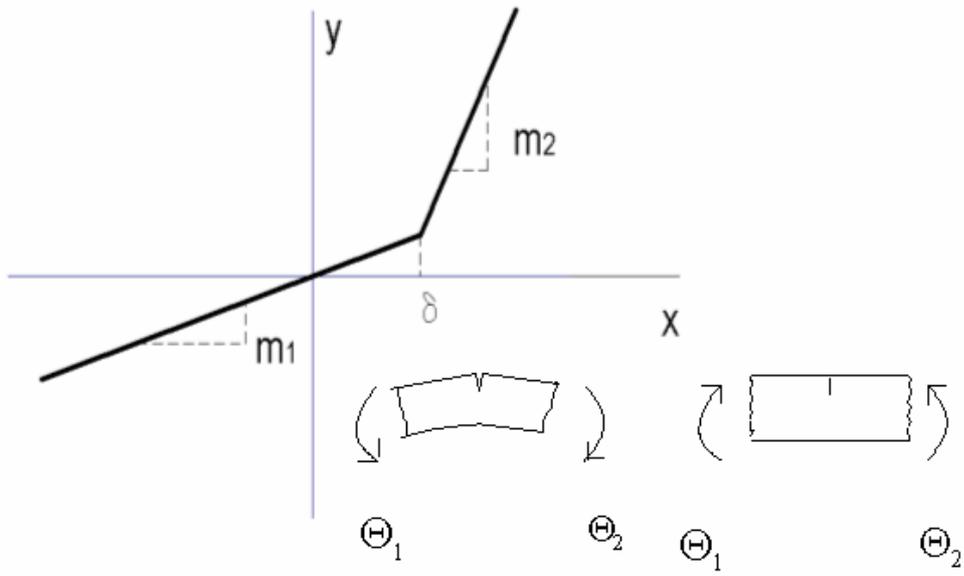
Figure 5.4 Bilinear crack model with crack closure effect,

crack is on the upper side of the beam

CHAPTER 6

CASE STUDIES AND DISCUSSION OF RESULTS

6.1 Introduction

In this part, several case studies are given to test and to demonstrate the applicability, efficiency and sensitivity of the method suggested. The crack is modelled as a bilinear crack having an asymmetric clearance caused by closure effects, as mentioned in the previous chapter.

In section 6.1, the applicability of the method suggested is sought by using a 3 dof cracked beam. In section 6.2, the locating sensitivity and the applicability of the method for different crack locations along the same beam are investigated by using a 6 dof cracked beam. The effect of the depth of the crack on localization of the crack is studied in section 6.3. In this section, a method for identification of the size of the crack is also suggested for specific structural components. And finally, in section 6.4, the applicability of the method for multiple cracks is studied.

6.2 Verification of the Method for Detecting Crack

The cracked cantilever beam, shown in Figure 6.1 is used to verify the method suggested in detecting cracks. The system has the following parameters (Case I):

Material   Aluminium

Young's modulus $E = 69.79 \cdot 10^9 \ \mathrm{N/m^2}$

Mass density $\rho = 2600 \ \mathrm{kg/m^3}$

Poison's ratio $v = 0.33$

Length of the beam. $l = 1.214 \ \mathrm{m}$

Width of the beam cross section $b = 50 \cdot 10^{-3} \ \mathrm{m}$

Depth of the beam cross section $h = 25 \cdot 10^{-3} \ \mathrm{m}$

Depth of the crack $a = 12 \cdot 10^{-3} \ \mathrm{m}$

Length of a beam finite element $L = 0.6107 \ \mathrm{m}$

Number of finite elements   2

Location of the crack   In the 2nd finite element.
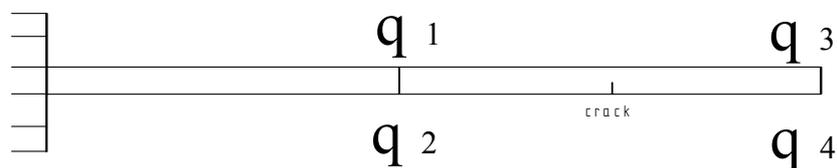
Figure 6.1 Cracked beam (4 dof)

First the dynamic response of the beam was calculated by using the method described in Section 5.2, at frequencies between 80 rad/sec and 100 rad/sec. Then at each frequency considered, nonlinearity numbers (NLNs) for all coordinates were calculated. The results are given in Figure 6.2.
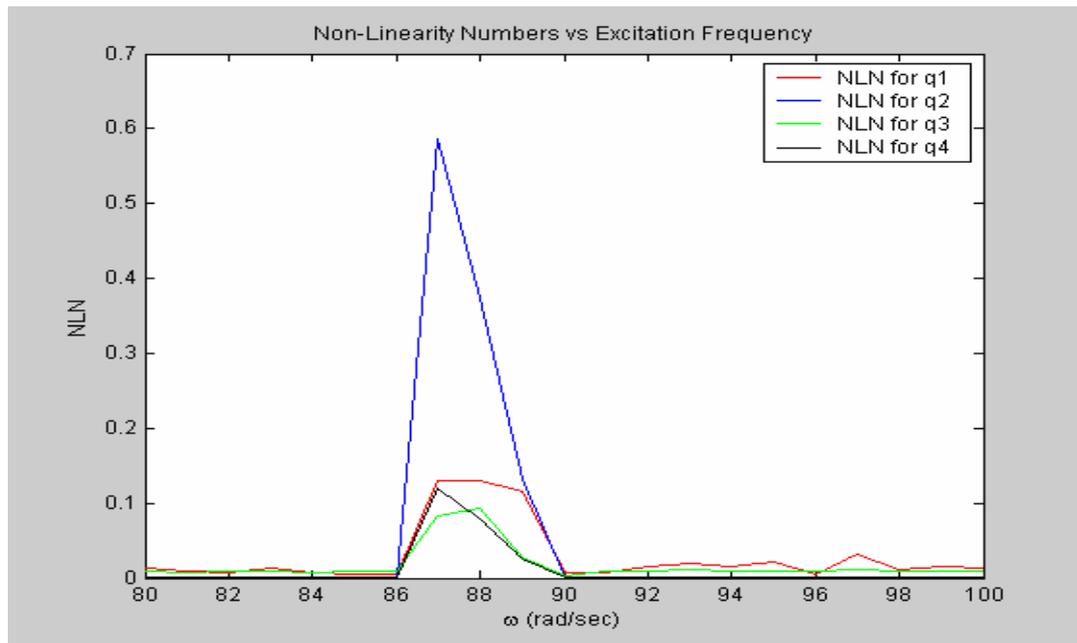
Figure 6.2 NLN for cracked beam ($Q_1 = F_1 = 5$ N)

As shown in the figure, the system has non-zero NLNs at all coordinates around 88 rad/sec which is the first natural frequency of the beam. Here we see that non-zero NLNs can be observed only around a resonance frequency. Furthermore, since the crack is in the second finite element, NLN for each coordinate of this element has a nonzero value, which is an expected result. It is also observed that most significant NLN belongs to the rotational coordinate q_2,

and the NLNs corresponding to a translational coordinates, namely q_1 and q_3, and the NLN for rotational coordinate q_4 are not as large as the NLN for rotational coordinate q_2.

As the forcing level is increased to Q_1=10 N, it's observed that NLN's increase, as shown in Figure 6.3, but the same general observations still apply.
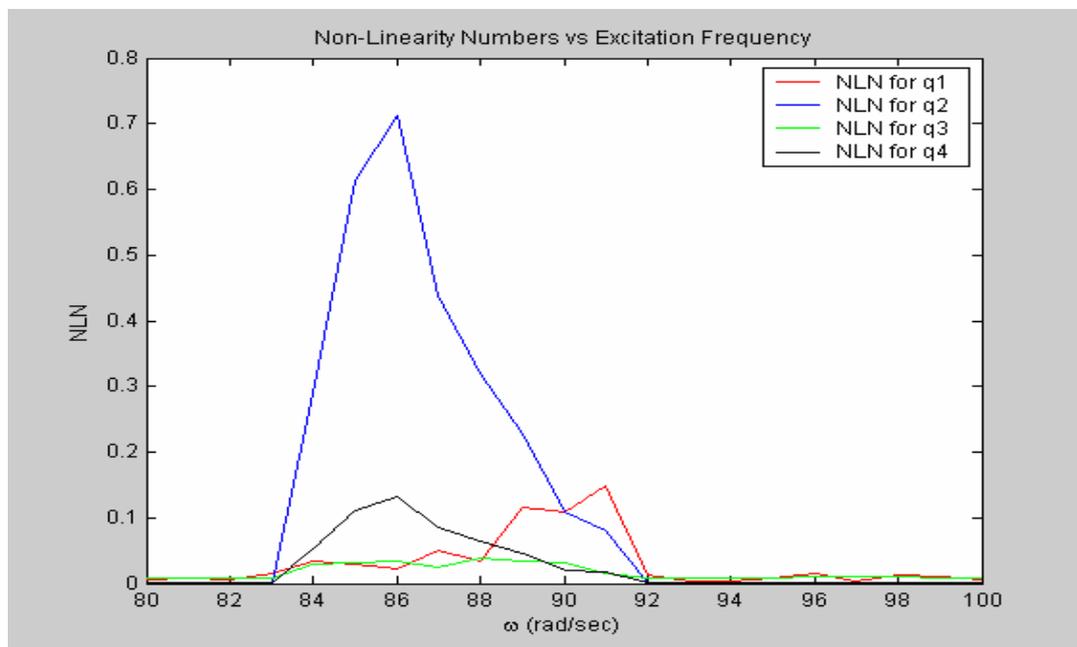
Figure 6.3 NLN for cracked beam under harmonic force of (Q_1=F_1=10 N)

In Figures 6.4 and 6.5, NLNs of the same coordinates to moments of magnitudes 1 N.m and 1.5 N.m, respectively, are plotted. The moments are applied at coordinate q_2. From these graphs, it can be easily seen that, NLNs for the rotational coordinate q_2 is higher in magnitude compared with other NLNs. By

comparing the shapes of the NLN curves around their peak points in Figures 6.2 and 6.3 with those in Figures 6.4 and 6.5, it can be concluded that NLNs of the rotational coordinates obtained by the rotational excitation of the cracked beam is much more effective and indicative for detecting the crack. In addition, NLNs for translational coordinates obtained by rotational excitation may also be used for detecting cracks. However, NLNs for translational coordinates obtained by translational excitation (not given here) may yield misleading results and may not be used for the detecting and locating purposes of cracks in beams.
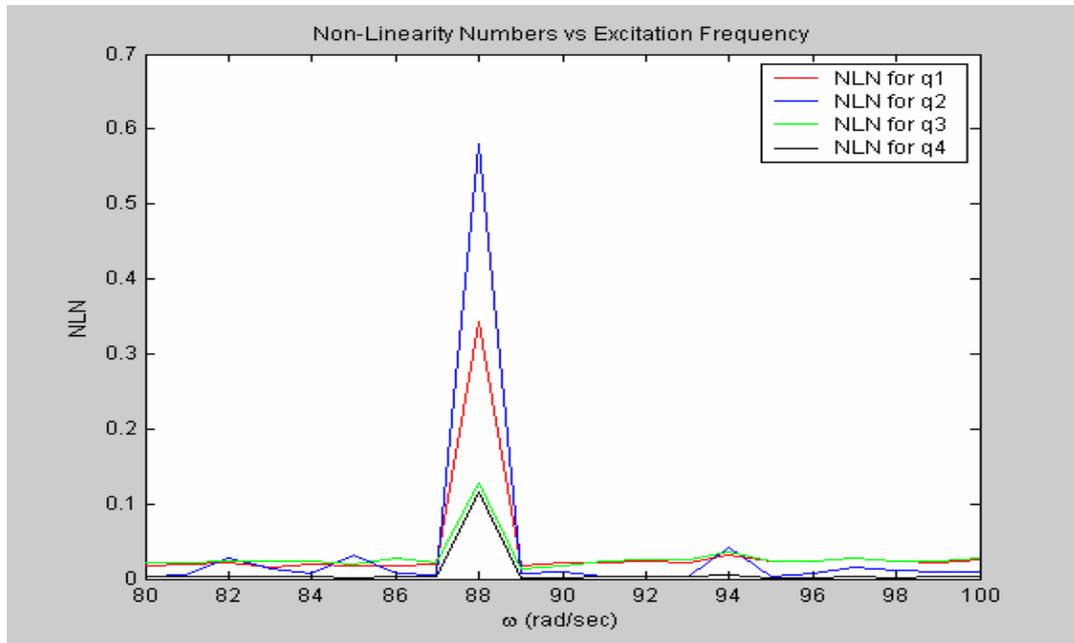
Figure 6.4 NLN for cracked beam ($Q_2=T_1=1$ N.m)
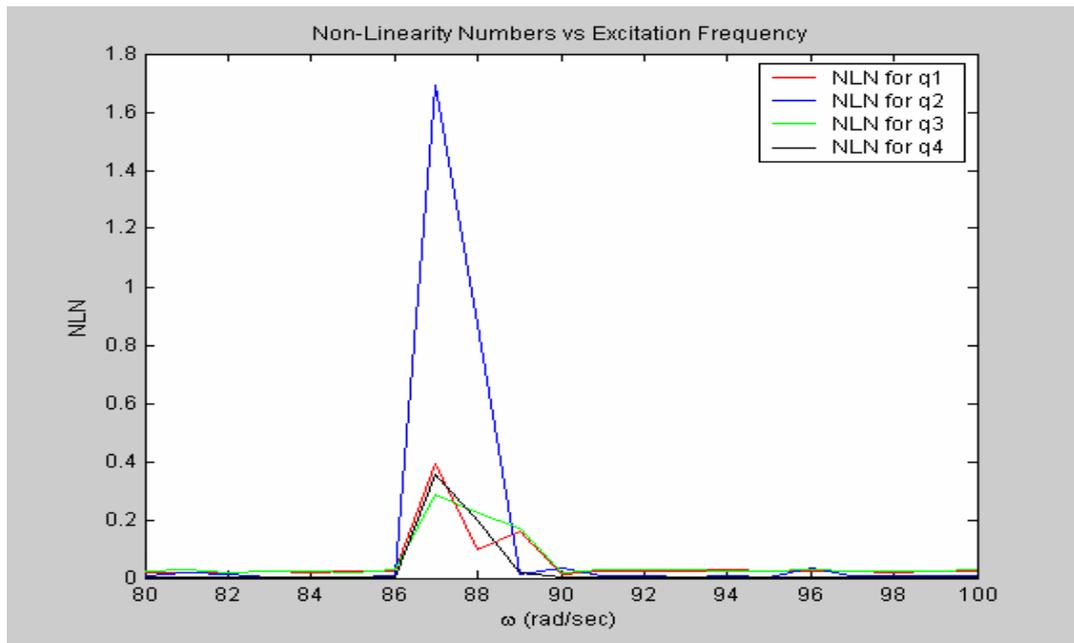
Figure 6.5 NLN for cracked beam ($Q_2 = T_1 = 1.5$ N.m).

It is inevitable to have some degree of measurement error in all measurements. In order to observe the effect of measurement errors, the beam response data is polluted by multiplying the calculated receptance values by random numbers (generated by Matlab R13 ®. function "randn") with a mean of 1 and standard deviation of 0.03. Thus, measurement errors with standard deviation of 3% are imposed into the simulated measurement values. Then, in order to study the effect of using simulated measurement results with some error, NLNs are calculated for both a cracked and uncracked beams. In Figures 6.6 and 6.7, NLNs for only rotational coordinates are shown for both cracked and uncracked beams by exciting the system with a transverse force ($Q_1 = 5$ N) and a moment ($Q_2 = 1$ N.m), respectively. NLNs obtained for uncracked beam are almost all zero, while

the cracked beam gives significant values, at the same excitation levels for the

rotational coordinates q_2 and q_4.
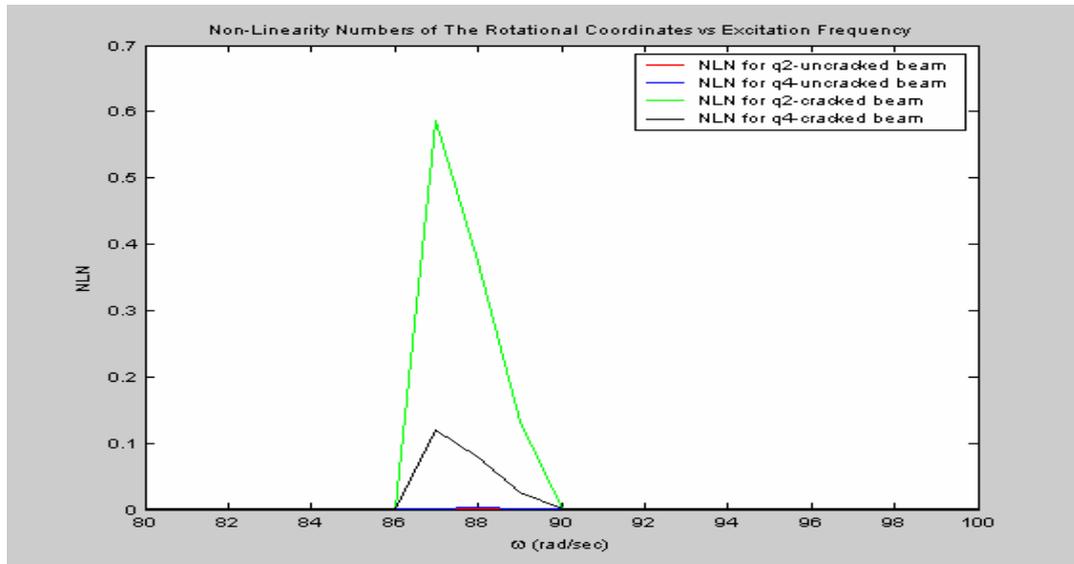
Figure 6.6 NLN for cracked and uncracked beam
(gathered by polluted receptance signal) $(Q_1 = F_1 = 5 \text{ N})$
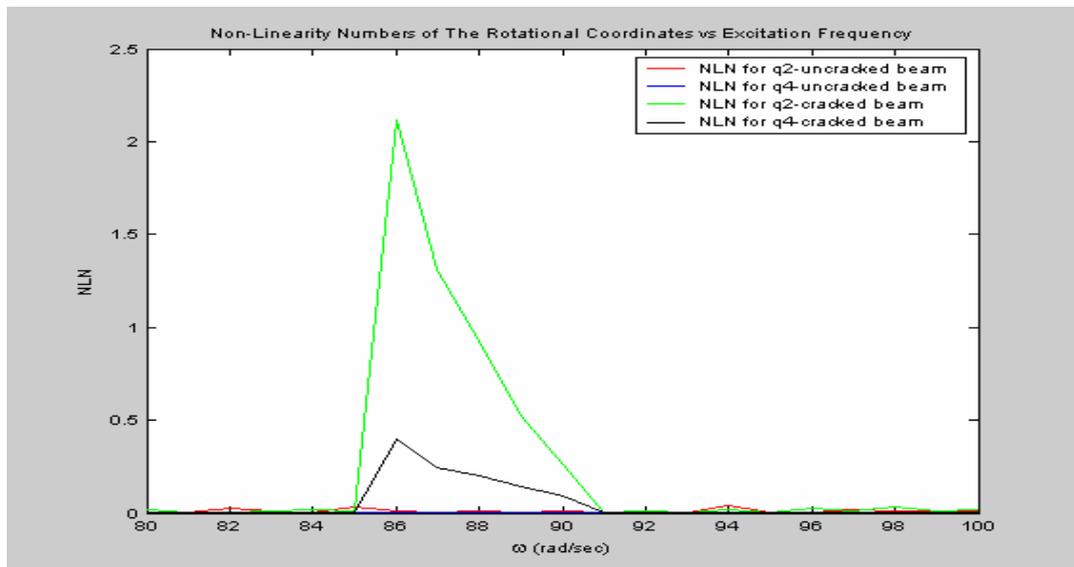
Figure 6.7 NLNs for cracked and uncracked beams
(gathered by polluted receptance signal) $(Q_2 = T_1 = 1 \text{ N.m})$

6.3 Determining Crack Location

In this section, the method developed is used to determine the crack location. In order to illustrate the application of the method for determining the crack location, three case studies are given.

The cracked beam used in these case studies has the following parameters.

Material	Aluminium
Young's modulus	$E = 69.79 \cdot 10^9 \ \text{N/m}^2$
Mass density	$\rho = 2600 \ \text{kg/m}^3$
Poison's ratio	$v = 0.33$
Length of beam.	$l = 1.214 \ \text{m}$
Width of beam	$b = 50 \cdot 10^{-3} \ \text{m}$
Depth of beam	$h = 25 \cdot 10^{-3} \ \text{m}$
Depth of crack	$a = 12 \cdot 10^{-3} \ \text{m}$
Length of beam element	$L = 0.4071 \ \text{m}$
Number of finite elements	3
Location of the crack	in the 1st finite element (Case II)
	in the 2nd finite element (Case III)
	in the 3rd finite element (Case IV)

CASE II:

The crack is inserted into the 1st finite element at the lower part of the beam with a depth of a=h/2=$12 \cdot 10^{-3}$ m (Figure 6.8). The beam is excited at the rotational coordinate q_6, from the free end of the beam. Four different forcing values were tested: Q_6=0.25 N.m, Q_6=0.35 N.m, Q_6=0.5 N.m, and Q_6=1 N.m. It was observed that for Q_6=0.25 N.m and for Q_6=0.35 N.m, the nonlinearity caused by the crack was not excited and did not yield an observeable difference between the receptance values at these two different forcing levels. Therefore, these are taken as the low forcing level measurement results. However, for Q_6=0.5 N.m, and Q_6=1 N.m, the nonlinearity is excited and the values are used as the high forcing measurements and NLNs of the structure were calculated basing on these results (Figure 6.9).
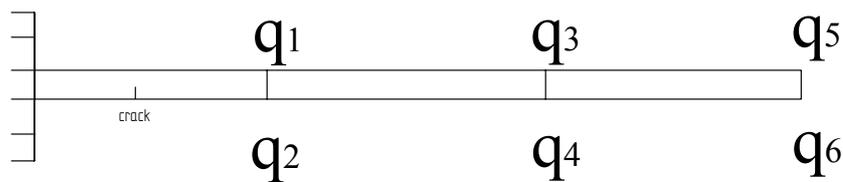
Figure 6.8 6 dof cracked beam (Case II)

As it can be seen from Figure 6.9, NLN of q_4 and q_6 have almost zero values when compared to the that of q_2. This clearly indicates that there is a nonlinearity

in the beam specimen connected to the 2nd coordinate only. Thus it illustrates that the method can successfully be used to locate the location of the crack on the beam.
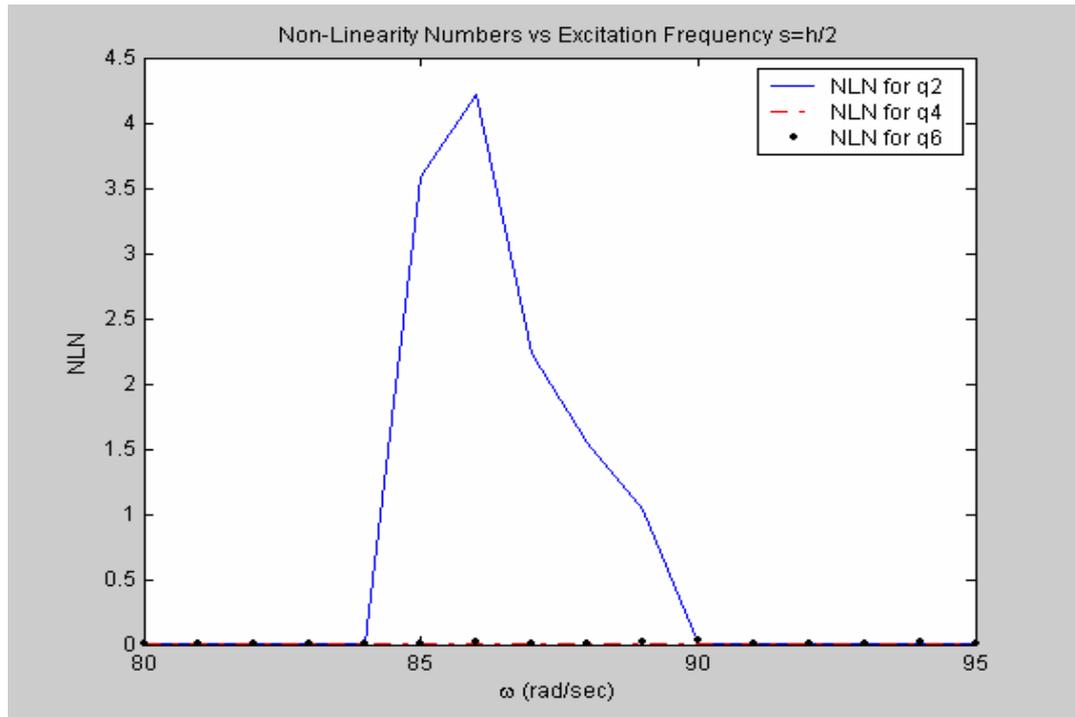
Figure 6.9 NLN graph for 6 dof beam model (Q_6=0.5 N.m)

CASE III:

In this case study, the crack is inserted in the 2nd finite element at the lower part again with a depth of a=h/2=$12 \cdot 10^{-3}$ m (Figure 6.10). The excitation levels are all kept the same as the previous case study and NLNs of the structure were calculated (Figure 6.11).
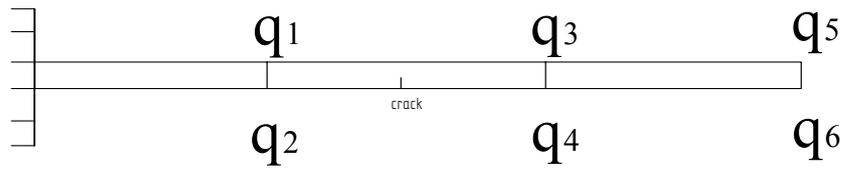
Figure 6.10 6 dof cracked beam (Case III)

NLN for q_2 and q_4 have almost the same values and also much higher compared to NLN of q_6. This denotes that there is a nonlinearity in the system and have connections with these two coordinates, q_2 and q_4. From Figure 6.11, the crack can be located in between the rotational coordinates q_2 and q_4, that is at the 2nd finite element.
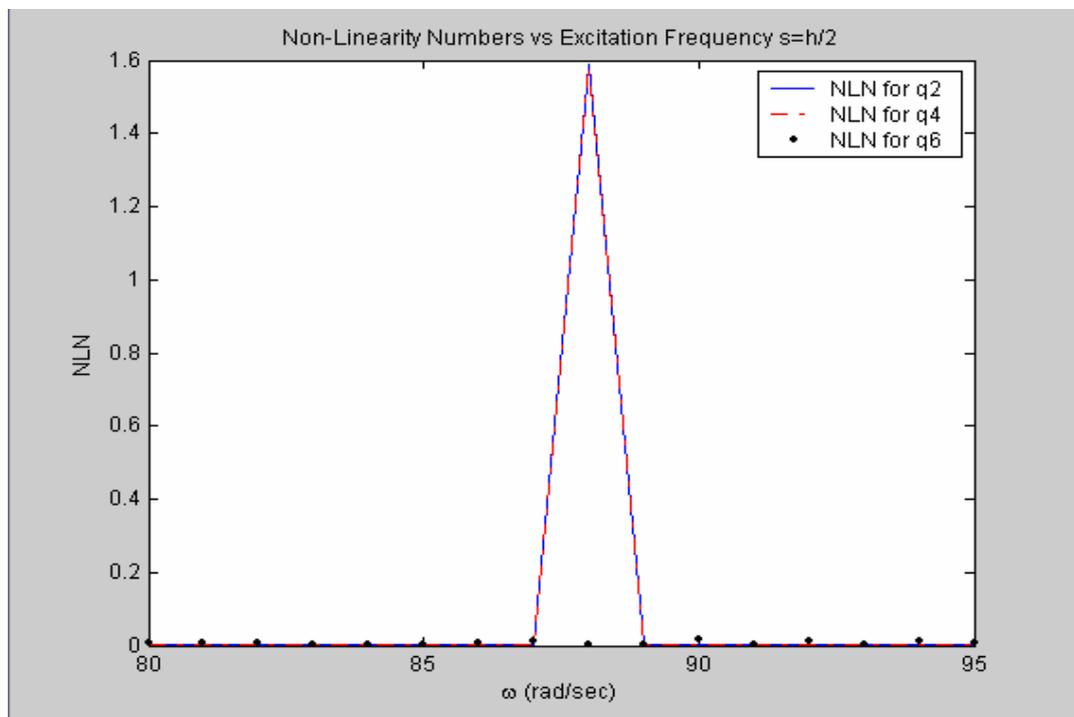
Figure 6.11 NLN graph for 6 dof beam model (Q_6=0.5 N.m)

CASE IV:

In this simulation, crack is inserted in the 3rd finite element at the lower part of the beam again with a depth of s=h/2=12·10^{-3} m (Figure 6.12). The excitation levels are all kept the same as before, and NLNs of the structure were calculated in the same range of frequencies (Figure 6.13).

q_1 q_3 q_5

crack

q_2 q_4 q_6
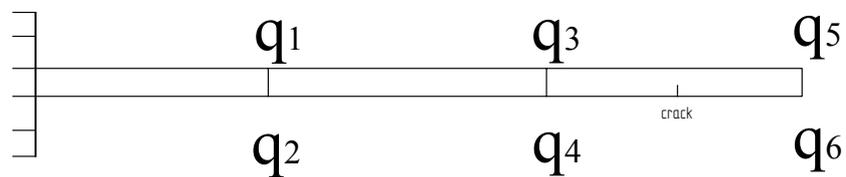
Figure 6.12 6 dof cracked beam (Case IV)
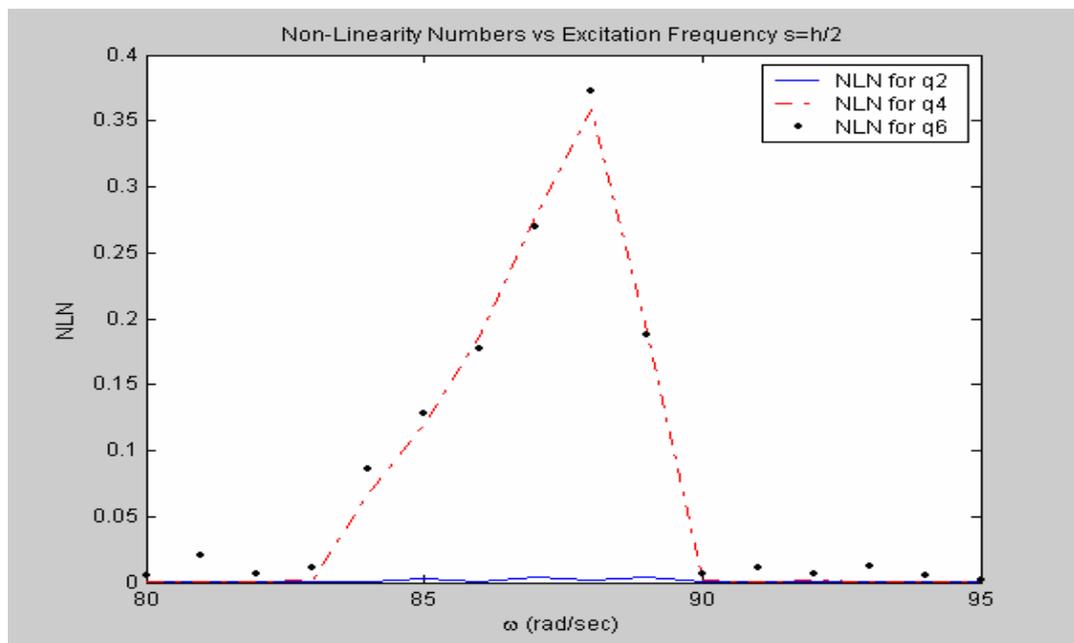
Figure 6.13 NLN graph for 6 dof beam model

From Figure 6.13, the crack can easily be located between coordinates q_4 and q_6, which means that the crack is in the 3rd finite element.

By examining Figures 6.9 of Case II, 6.11 of Case III and 6.13 of Case IV, a trend of decrease in NLN values can be observed. The maximum NLN is observed when the crack is in the 1st element, and the minimum value is obtained when it is in the 3rd element. This is an expected observation since for all cases (Case II, Case III and Case IV) the beam is excited from the free end, which causes a large moment at the cantilevered side that leads to a maximum excitement of the nonlinearity caused by the crack in the first element. So, observing the maximum value of NLN in Case II is an expected result.

6.4 Effect of Crack Depth on Localization

In this section, the effect of the crack depth on the localization is studied with numerical case studies.

The depth of the crack is given values $a \cong h/2 = 12 \cdot 10^{-3}$ m, $a \cong h/4 = 6 \cdot 10^{-3}$ m, $a \cong h/8 = 3 \cdot 10^{-3}$ m and $a \cong h/16 = 1.5 \cdot 10^{-3}$ m for the systems in Case II, Case III and Case IV. The NLN graphs for rotational coordinate q_2 in

Case II, rotational coordinate q_4 in Case III and rotational coordinate q_6 in Case IV are given for the crack depths mentioned above, in Figures 6.14, 6.15 and 6.16, respectively.

Note that the coordinate from which we can detect the crack is used in each case. If it can be detected from the NLN for more than one coordinate, then the one which gives the best indication is used in the following analysis.

It is also interesting to observe softening spring effect from the Figure 6.14 below. The beam has its 1st natural frequency at 88 Hz, however, as the severity of nonliearity is increased by the depth of the crack, NLN curve tends to move left, shifting the peak point on frequency axis.
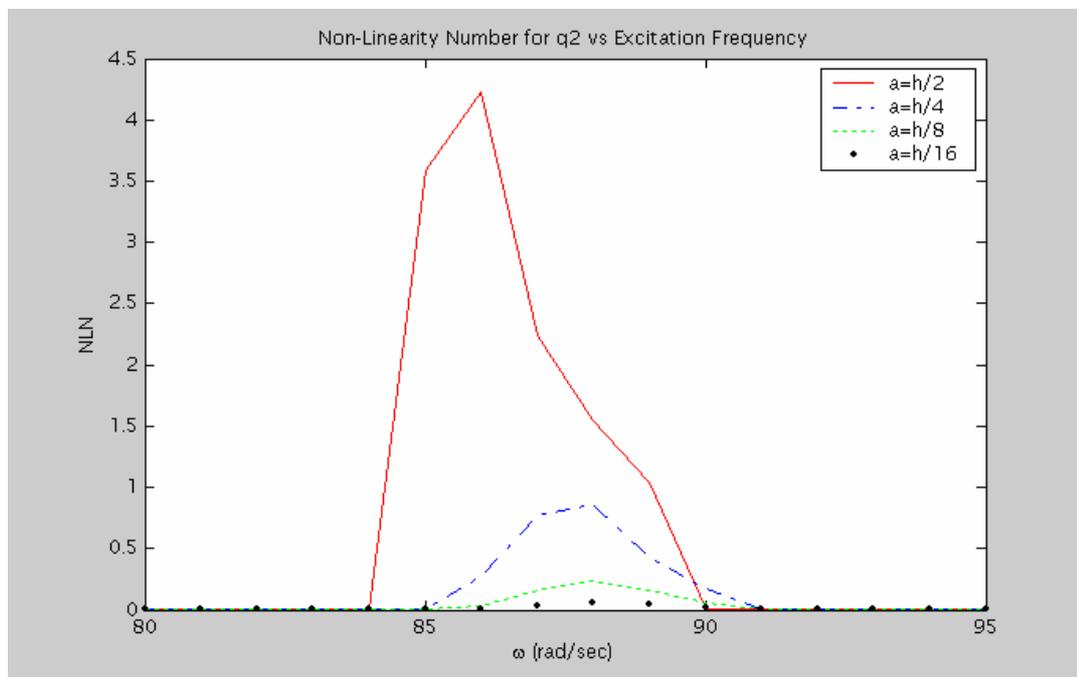
Figure 6.14   NLN graph for q$_2$ (CaseII) with various crack depths
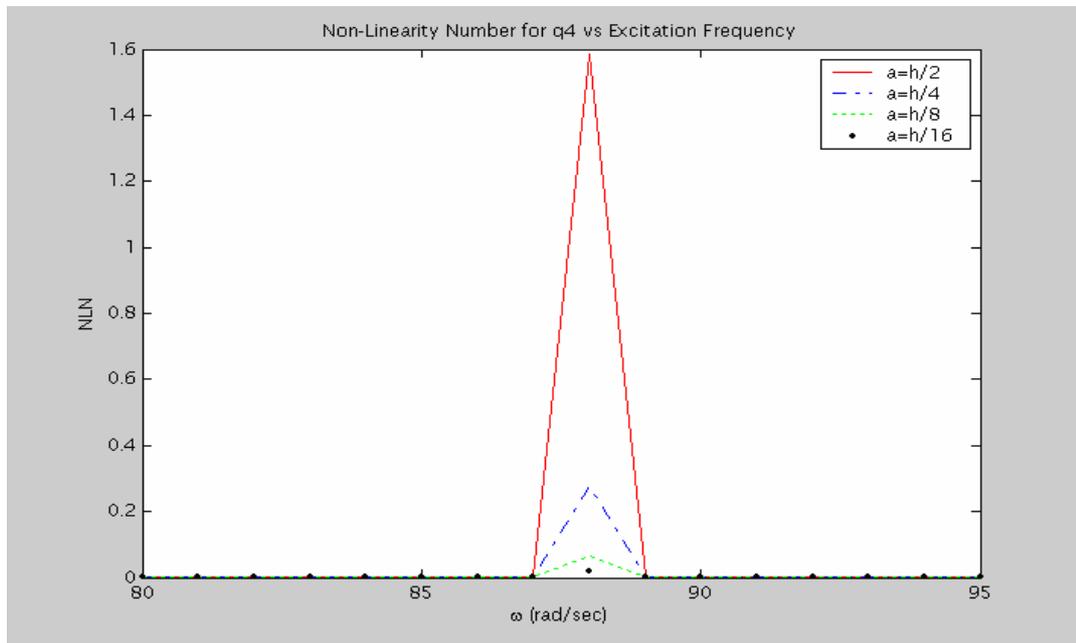
Figure 6.15   NLN graph for q2 (CaseIII) with various crack depths
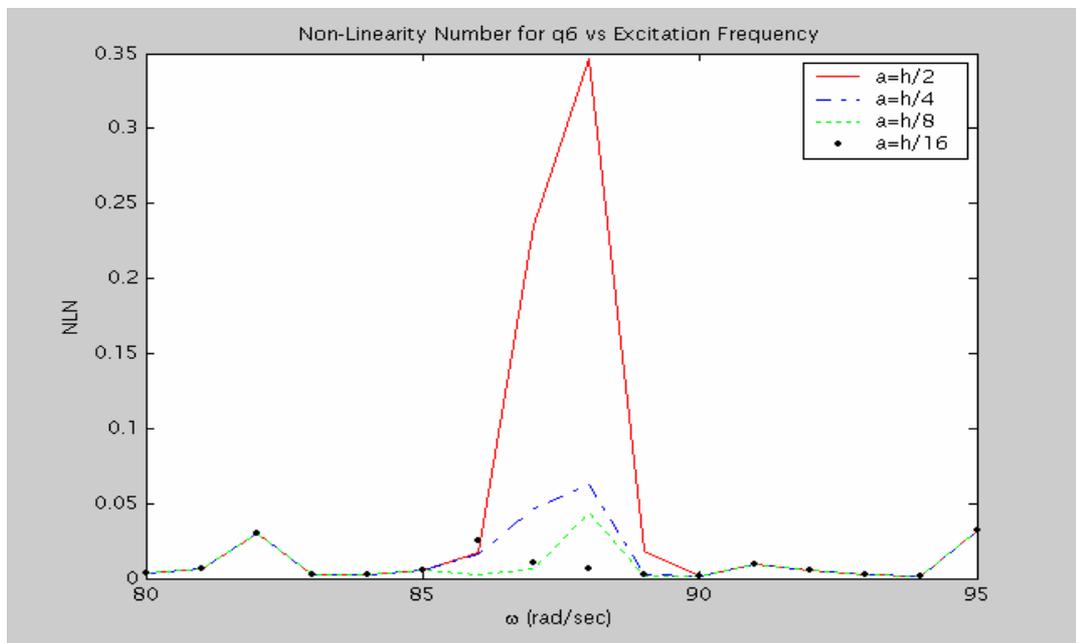
Figure 6.16   NLN graph for q2 (CaseIV) with various crack depths

When the depth of the crack is reduced, the location of the crack can still be determined; however smaller NLN will be obtained indicating that crack is smaller. Since NLN is a quantity that strongly depends upon the degree of nonlinearity in the structure, reduction in crack depth will reduce NLN as well. This means that it will be harder to detect and locate the crack when the crack depth is very small.

For specific structural components, dimensionless NLN charts may be constructed in order to detect, locate and even quantify the extent of damage. For example, from the NLNs of the interested beam for various crack depths and various crack locations, following chart can be constructed from the numerical results obtained:

Crack depth ratio	Case II	Case III		Case IV	
	NLN of q2	NLN of q2	NLN of q4	NLN of q4	NLN of q6
2	4.223	1.589	1.584	0.345	0.346
4	0.857	0.271	0.275	0.066	0.062
8	0.241	0.066	0.066	0.015	0.017
16	0.061	0.017	0.017	0.006	0.007

The 1st column of NLN values (of q$_2$) are obtained from Case II, the 2nd and the 3rd columns of NLN values (of q$_2$ and q$_4$) are obtained from Case III and the 4th and the 5th columns of NLN values (of q$_4$ and q$_6$) are obtained from Case IV. Crack depth ratio is the ratio of the height of the cross section of the beam to depth of crack. By obtaining such a table for a specific component and using it as a master, it may be possible to identify crack sizes in similar components.

The NLN values in the 1st, 3nd and 5th columns of Table 6.1 corresponding to the coordinates q$_2$, q$_4$ and q$_6$ respectively, are plotted versus dimensionless crack depth ratio in Figures 6.17, 6.18 and 6.19 in log-log scale.
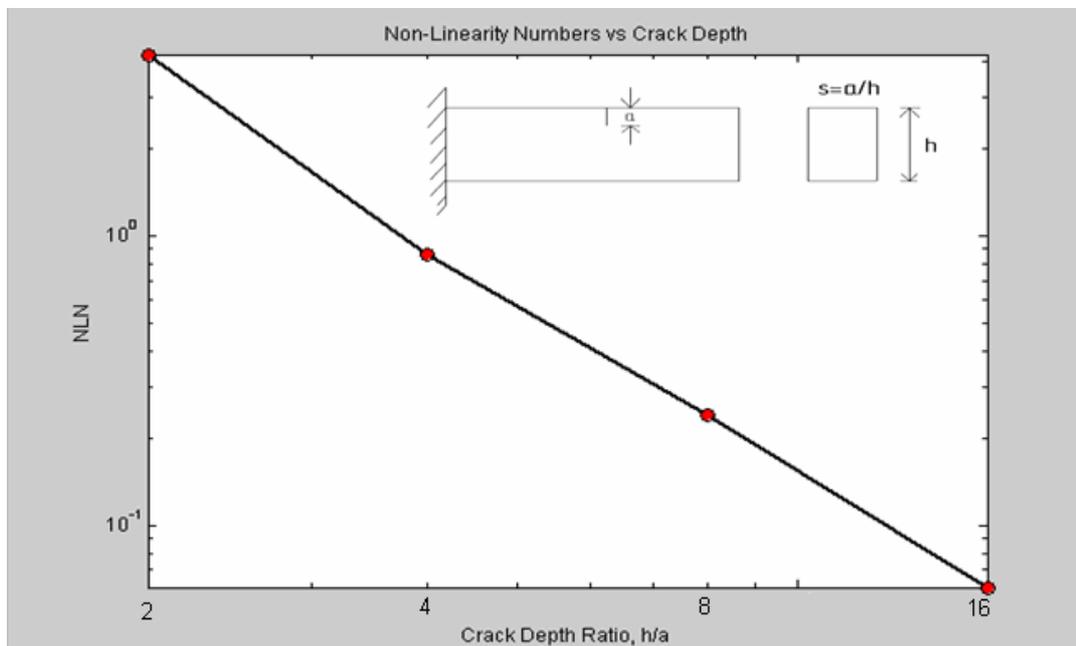
Figure 6.17 Variation of NLN with crack depth ratio (Case II.)
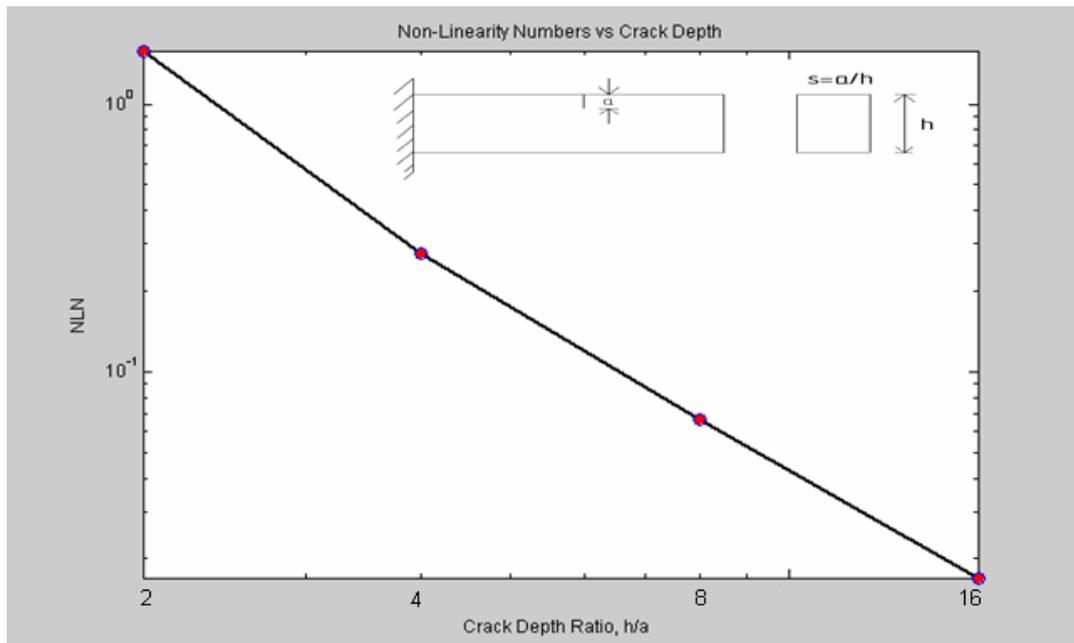
Figure 6.18 Variation of NLN with crack depth ratio (Case III)
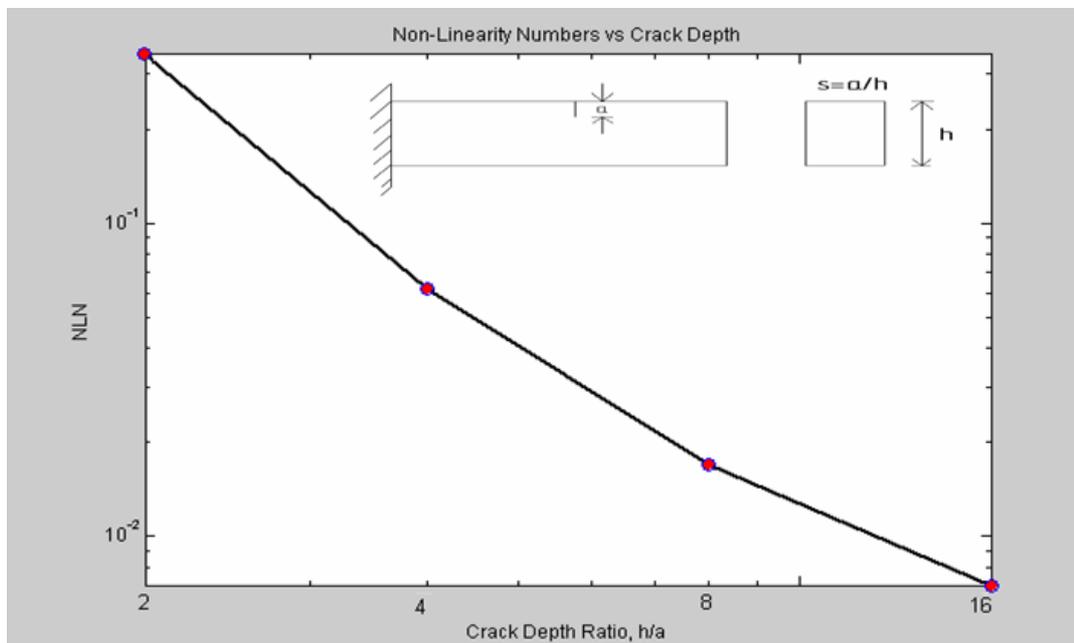
Figure 6.19 Variation of NLN with crack depth ratio (Case IV).

The curves obtained, in all three cases (Case II, Case III, and Case IV), are almost straight lines, which is quite interesting. This property can also be used to identify the magnitude of the size of the crack, in the presence of such master curves for specific structures.

6.4 The Effects of Multiple Cracks In Beams

In this section, the effects of multiple cracks in a structure is investigated. The cracked beam used in the case study has the following parameters (Figure 6.20):

Material	Aluminium
Young's modulus	$E = 69.79 \cdot 10^9 \ \text{N/m}^2$
Mass density	$\rho = 2600 \ \text{kg/m}^3$
Poison's ratio	$v = 0.33$
Length of the beam.	$l = 1.214 \ \text{m}$
Width of beam	$b = 50 \cdot 10^{-3} \ \text{m}$
Depth of beam	$h = 25 \cdot 10^{-3} \ \text{m}$
Depth of crack	$a = 12 \cdot 10^{-3} \ \text{m}$
Length of the beam element	$L = 0.2036 \ \text{m}$
Number of finite elements	6
Location of the crack	in the finite 1$^{\text{st}}$ element and in the 3$^{\text{rd}}$ finite element at the same time.
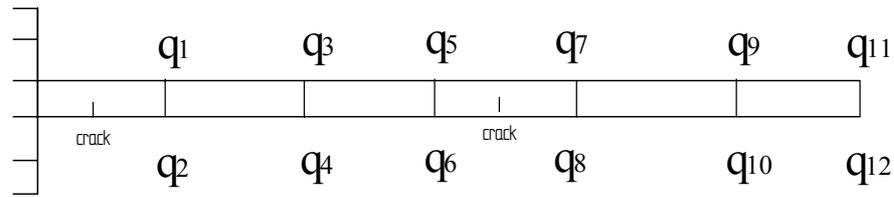
Figure 6.20 12 dof cracked beam

There exist two cracks in the beam specimen, one is in the 1st finite element at the lower part of the beam and the other is in the 3rd finite element at the lower part of the beam. Both has a depth of $a=h/2=12\cdot10^{-3}$ m. The beam is excited at the rotational coordinate q_{12}, from the free end of the beam. When, as an excitation moment the following values are used: $Q_{12}=0.25$ N.m, $Q_{12}=0.5$ N.m, $Q_{12}=1$ N.m, $Q_{12}=1.5$ N.m, $Q_{12}=2$ N.m. and $Q_{12}=2.5$ N.m. For $Q_{12}=0.25$ N.m and $Q_{12}=0.5$ N.m, none of the the nonlinearities caused by the crack were excited; and therefore no observeable differences between the receptance values of the any coordinates were recorded. Therefore, these are taken as the low forcing levels measurement results. However, for $Q_{12}=1$ N.m, $Q_{12}=1.5$ N.m, $Q_{12}=2$ N.m and $Q_{12}=2.5$ N.m, the 1st nonlinearity is excited and these values are considered as the high forcing measurements.

The NLN curves of the rotational coordinates q_2, q_4, q_6, q_8, q_{10} and q_{12} are plotted at five different forcing levels mentioned above in Figure 6.21. It can be concluded from the study of figure that there are cracks in the 1st finite element located between q_2 and the ground and also in the 3rd finite element located

74

between q_6 and q_8, from the fact that NLNs for these coordinates are nonzero around resonance. Although the 1st crack reveals itself at the forcing level of Q_{12}=1 N.m, the 2nd crack reveals its position on the beam when Q_{12}=2N.m.
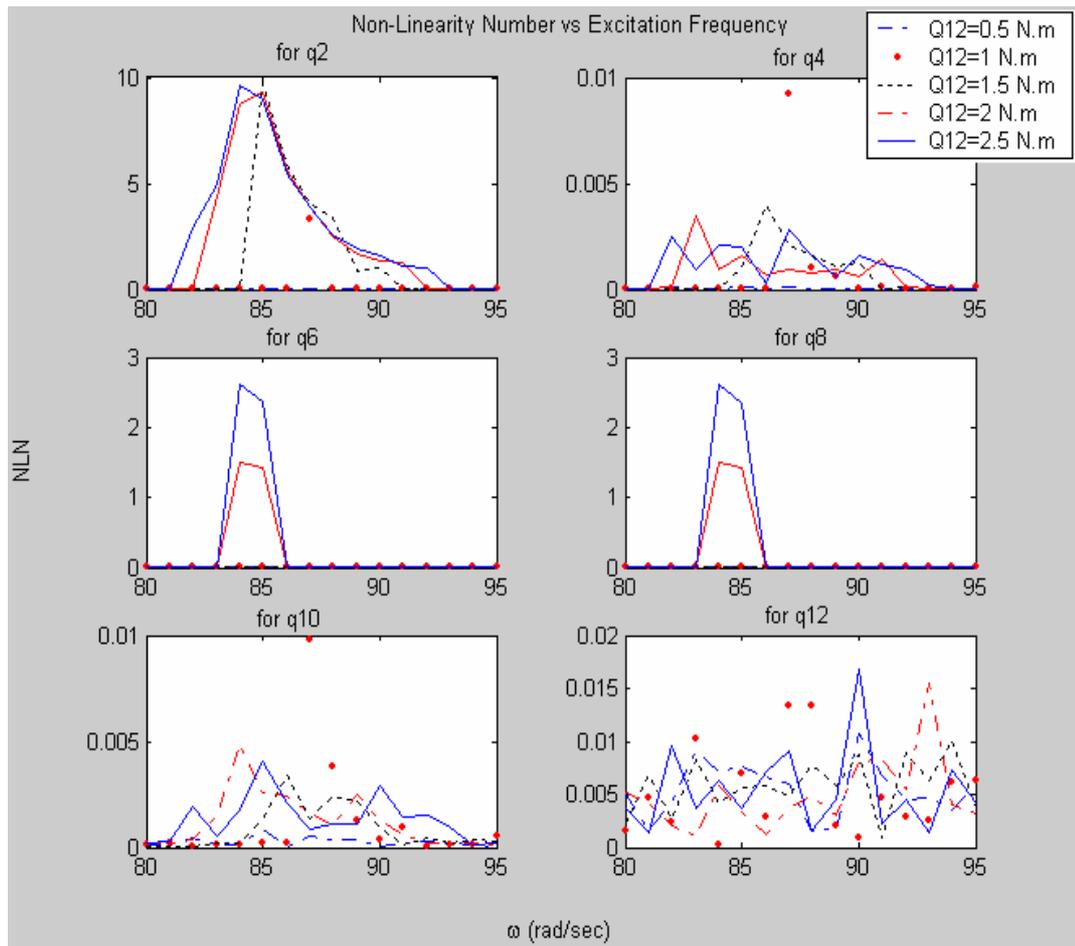
Figure 6.21: NLN graph for 12 dof beam model

CHAPTER 7

CONCLUSIONS AND RECOMMENDATIONS

In this thesis, detection and localization of cracks in structural systems from measured frequency response functions is studied. The method developed uses the experimentally measured receptances at different forcing levels as input, and gives the location of the crack as output, if it exists. The principle behind the method presented is that vibration signature (frequency response function) data is a sensitive indicator of structural integrity and may be exploited to detect, locate and even identify a damage, which creates nonlinearity.

It is well known that, when a structural component has a crack, then the crack induces a local flexibility. This flexibility is a function of crack depth, therefore it alters the dynamic behaviour of the structure itself. In most of the previous work on the subject, the effect of crack on natural frequencies and mode shapes of the structure has been studied. In this study, however, detection and localization of a crack is aimed by using frequency response of the system at

different forcing levels.

The method suggested is an extension of the method recently developed in a previous study. In order to verify the method suggested for detection and locating a crack type damage, the time simulation for cracked beams are made at several different excitation frequencies around the first resonant frequency so that nonlinear frequency response characteristics of damaged systems were obtained. Then this data are used in the method suggested as if they were experimentally obtained.

Several case studies are performed to demonstrate the applicability of the technique. Case studies performed indicate that frequency response functions of rotational coordinates give the best results for crack detection when compared to those of translational counterparts. Similarly, using rotational excitation rather than translational one is much more effective and indicative for detection of cracks.

The locating sensitivity of the method is also examined for different crack locations by several case studies. It is found that excitation point is also very important to detect cracks in beams. The method gives indicative results when the excitation point is selected such that the excitation excites the nonlinearity caused by the crack on beam.

The effect of the depth of the crack on localization of the crack is also studied. It is found that it becomes harder to detect and locate the crack when crack depth is small. This is so because the reduction in crack depth reduces the degree of nonlinearity in beam caused by crack.

For the identification of the size of a crack, drawing a chart is suggested. For specific structural components, dimensionless charts may be constructed to quantify the extent of damage present in the structure. This kind of charts may be formed as a result of experiments done for different important and critical crack sizes and crack locations on that specific structures. The method bases on an interesting feature observed between NLN and size of the crack: logarithm of NLN is changing linearly with the logarithm of the depth of a crack.

One important outcome of the case studies is that the method suggested is also applicable when there exists multiple cracks in the structure. The method is capable of detecting and finding locations of the cracks in this case as well.

It should be noted that single harmonic describing functions are used in the method suggested. The method presented is capable of detecting and locating the crack even only with that fundamental harmonic. However, it is also possible to include higher harmonics in the calculations which may improve the results, in the

expense of increasing the computation effort. During the time simulations of the cracked beams in case studies, it is observed that time responses include significant second harmonic components and noticeable bias terms when the excitation frequency is about half of the natural frequency of the beam. When it is dangerous to performe experiments around the first natural frequency, this feature may be exploited and the NLN can be extracted from the experiments around half of the first natural frequency. In this case, beside the first, zeroth and second harmonic describing functions must also be calculated.

The technique can further be extended to include parametric identification of cracks in order to predict crack parameters, such as depth of crack. Since the type of the nonlinearity to be searched for is known, the nonlinearity matrix Δ, which has the damage information in it, may be constructed by dual input describing function concept (given at the appendix A) with unknown bilinear stiffness parameters and may be substituted into the Equation (5.7). Then, all the algebraic equations obtained can be optimized to calculate the bilinear stiffness parameters. For the optimization, either singular value decomposition or any other optimization method can be used. From the bilinear stiffness parameters, with an inverse calculation using the Equations (3.1) to (3.21), the depth of the crack may be calculated. In addition to dual input, including second harmonic describing function may also improve the accuracy of the identification procedure.

Neural network approach, which is widely used in crack detection applications [57-62], may also be adapted with the method suggested for the identification purposes.

Finally, it may be claimed that the method developed may also be extended to detect, locate and quantify the cracks in rotating structural components, which is an important subject in crack detection [64-67].

REFERENCES

[1]   S. W. Doebling, C. R. Farrar, M. B. Prime and D. W. Shevitz, "Damage Identification and Health Monitoring of Structural and Mechanical Systems from Changes In Their Vibration Characteristics; a Literature Review", Report No: LA-13070-MS, Los Alamos National Laboratory, 1996.

[2]   A. Rytter, "Vibration Based Inspection of Civil Engineering Structures", Ph. D. Dissertation, Department of Building Technology and Structural Engineering, Aalborg University, 1993.

[3]   F. Leonard, J. Lanteigne, S. Lalonde and Y. Turcotte, "Free Vibration Behaviour of a Cracked Cantilever Beam and Crack Detection", Mechanical Systems and Signal Processing, 15, 529-548, 2001.

[4]   G.- L. Qian, S. -N. Gu, J. -S. Jiang, "The Dynamic Behaviour and Crack Detection of a Beam with a Crack", Journal of Sound and Vibration, 138, 233-243, 1989.

[5]   P. F. Rizos, N. Aspragathos, A. D. Dimarogonos, "Identification of Crack Location & Magnitude in a Cantilever Beam from the Vibration Modes", Journal of Sound and Vibration 138, 381-388, 1990.

[6]   W. M. Ostachowicz and M. Krawczuk, "Vibration Analysis of a Cracked Beam", Computers and Structures, 36, 245-250, 1990.

[7]   W. M. Ostachowicz and M. Krawczuk, "Analysis of the Effect of Cracks on the Natural Frequencies of a Cantilever Beam", Journal of Sound and Vibration, 150,191-201, 1991.

[8]   T. Y. Kam, T. Y. Lee, "Detection of cracks in structures using modal test data", Engineering Fracture Mechanics, 42, 381-387. 1992.

[9]   D. Armon, Y. B.-Haim, S. Braun, "Crack Detection in Beams by Rank-Ordering of Eigenfrequency Shifts", Mechanical Systems and Signal Processing, 8, 81-91, 1994.

[10]   Y. Narkis, "Identification of Crack Location in Vibrating Simply Supported Beams", Journal of Sound and Vibration, 172, 549-558, 1994.

[11]   J.N. Sundermeyer and R.L. Weaver, "On Crack Identification and Characterization in a Beam by Nonlinear Vibration Analysis", Journal of Sound and Vibration 183, 857-871, 1995.

[12]   A. D. Dimarogonos, "Vibration of Cracked Structures: State of Art Review", Engineering Fracture Mechanics, 55, 831-857,1996.

[13]   R. Ruotolo, C. Surace, P. Crespo, D. Storer, "Harmonic Analysis of the Vibrations of a Cantilever Beam with a Closing Crack", Computers&Structures, 61, 1057-1074, 1996.

[14]   R. Ruotolo and C. Surace, "Damage Assessment of Multiple Cracked Beams: Numerical Results & Experimental Validation", Journal of Sound and Vibration, 206, 567-588, 1997.

[15]   B.P Nandwana and S.K. Maiti, "Detection of the Location & Size of a Crack in Stepped Cantilever Beam Based on Measurements of Natural Frequencies", Journal of Sound and Vibration, 203, 435-446, 1997.

[16]   M. Chati, R. Rand and S. Mukherjee, "Modal Analysis of a Cracked Beam", Journal of Sound and Vibration, 207, 249-270, 1997.

[17]   T.G. Chondros, A. D. Dimarogonas, "A Continous Cracked Beam Vibration Theory, Journal of Sound and Vibration, 215, 17-34, 1998.

[18]   M. Boltezar, B. Strancar, A. Kuhelj, "Identification of Transverse Crack Location in Flexural Vibrations of Free-Free Beams", Journal of Sound and Vibration 211, 729-734, 1998.

[19]   A. Rivola and P.R. White, "Bispectral Analysis of the Bilinear Oscillator with Application to the Detection of Fatigue Cracks", Journal of Sound and Vibration, 216, 889-910, 1998.

[20]   S. Masoud, M.A. Jarrah and M. Al-Maamory, "Effect of Crack Depth on the Natural Frequency of a Prestressed Fixed-Fixed Beam", Journal of Sound and Vibration, 214, 201-212. 1998.

[21]   M. Cheng, X. J. Wu, W. Wallace, "Vibrational Response of a Beam with a Breathing Crack", Journal of Sound and Vibration, 225, 201-208, 1999.

[22]   E.I. Shifrin and R. Ruotolo, "Natural Frequencies of a Beam with an Arbitrary Number of Cracks", Journal of Sound and Vibration 222, 409-423, 1999.

[23]   S. Chinchalkar, "Determination of Crack Location in Beams Using Natural Frequencies", Journal of Sound and Vibration, 247, 417-429. 2001.

[24]   A.Z. Khan, A.B. Stanbridge and D.J. Ewins, "Detecting Damage in Vibrating Structures with a Scanning LDV", Optics and Lasers in Engineering, 32, 583-592. ", 2000.

[25]   Y.S Lee and C.J. Chung, "A Study on Crack Detection Using Eigenfrequency Data", Computers and Structures 77, 327-342, 2000.

[26]   S.L. Tsfansky and V.I.Beresnevich, "Nonlinear Vibration Method for Detection of Fatigue Cracks in Aircraf Wings" Journal of Sound and Vibration 236, 49-60, 2000.

[27]   N.T. Khiem and T.V. Lien, "A Simplified Method for Natural Frequency Analysis of a Multiple Cracked Beam", Journal of Sound and Vibration 245, 737-751, 2001.

[28]   G. Kerschen and J.C. Golinval, "Theoretical & Experimental Identification of a Nonlinear Beam", Journal of Sound and Vibration 244, 597-613., 2001.

[29]   E. Viola, l. Federici and L. Nobile, "Detection of Crack Location Using Cracked Beam Element for Structural Analysis", Theoretical and Applied Fracture Mechanics, 36, 23-35, 2001.

[30]   M. Krawczuk, "Application of Spectral Beam Finite Element with a Crack&Iterative Search Technique for Damage Detection", Finite Elements In Analysis and Design, 38, 537-548., 2002.

[31]   P. N. Saavedra, L. A. Cuitino, "Crack Detection&Vibration Behavior of Cracked Beam", Computers&Structures, 79, 1451-1459, 2001.

[32]   Q. S. Li, "Vibratory Characteristics of Multi-Step Beams with an Arbirary Number of Cracks and Concenrated Masses", Applied Acoustics, 62, 691-706., 2001.

[33]   J. K. Sinha, M. I. Friswell, S. Edwards, "Simplified Models for the Locations of Cracks in Beam Structures Using Measured Vibration Data", Journal of Sound and Vibration 251, 13-38, 2002.

[34]   J. K. Sinha, M. I. Friswell, "Simulation of The Dynamic Response of a Cracked Beam", Computers and Structures, 80, 1473-1476, 2002.

[35]   N. Pugno, C. Surace, "Evaluation of The Nonlinear Dynamic Response to Harmonic Excitation of a Beam Wtih Several Breathing Cracks", Journal of Sound and Vibration, 235, 749-762, 2000.

[36]   J. -T. Kim, Y. -S. Ryu, H. -M. Cho, N. Stubbs, "Damage Identification in Beam-Type Structures: Frequency-Based Method vs Mode-Shape-Based Method", Engineering Structures, 25, 57-67, 2002.

[37]   J. -T. Kim, N. Stubbs, "Crack Detection in Beam-Type Structures Using Frequency Data", Journal of Sound and Vibration, 259, 145-160, 2002.

[38]   K. Waldron, A. Ghoshal, M. J. Schulz, M. J. Sundaresan, F. Ferguson, P. F. Pai, J. H. Chung, "Damage Detection Using Finite Elements&Laser Operational deflection Shapes, Finite Elements in Analysis and Design, 38, 193-226, 2002.

[39]   H. J. Rice, "Identification of Weakly Nonlinear Systems Using Equivalent Linearization", Journal of Sound and Vibration, 185, 473-481, 1994.

[40]   R. M. Lin and D.J. Ewins, "Location of Localised Stiffness Nonlinearity Using Measured Modal Data", Mechanical Sstems and Signal Processing, 9, 329-339, 1995.

[41]   S. –S, Lee, Y. –S. Park, "Position of Nonlinear Elements and Identification of Their Type by a Local Non-Parametric Method", Mechanical Sstems and Signal Processing, 5, 403-420, 1991.

[42]   E. F. Crawley, A. C. Aubert, "Identification of Nonlinear Structural Elements by Force State Mapping", AIAA Journal, 24,155-162, 1986.

[43]   M. B. Özer and H.N. Özgüven, "Localization and Identification of Nonlinearity in Structures", Proceedings of ESDA2002, 2002.

[44]   M. Özer, "A New Method on Identification of Symmetrical Nonlinearities In Structures", MS. Thesis, Middle East Technical University, 1999.

[45]   D. Broek, "Elementary Engineering Fracture Mechanics", Dordrecht, 4th Edition, 1986.

[46]   A. D. Dimarogonas, S. A. Paipetis, Analytical Methods In Rotor Dynamics, Applied Science Publishers Ltd, 1983.

[47]   S. P. Timoshenko, J. M Gere, Mechanics of Materials, PWS Pub Co., 1997.

[48]   H. Tada, P. C. Paris, G. R. Irwin, "The Stress Analysis of Cracks Handbook", ASME Press, 3rd Edition, 2000.

[49]   W. T. Thomson, Theory and Vibration with Applications, 4th Edition, Chapman&Hall, 1997.

[50]   E. Budak, H.N. Özgüven, "Iterative Receptance Method for Determining Harmonic Response of Structures with Symmetrical Nonlinearities", Mechanical Systems and Signal Processing, 7 (1), 75-87, 1993.

[51]   E. Budak, "Dynamic Analysis of Nonlinear Structures for Harmonic Excitation", MS. Thesis, Middle East Technical University, 1989.

[52]   Ö. Tanrıkulu, B. Kuran, H.N. Özgüven, M. İmregün, "Forced Harmonic Analysis of Nonlinear Structures Using Describing Functions", AIAA Journal, 31,1313-1320, 1993.

[53]   Ö. Tanrıkulu, "Forced Periodic Response Analysis of Nonlinear Structures", Imperial College of Science, Technology and Medicine, 1991.

[54]   A. Gelb, W. E. Vander Velde, "Multiple Input Describing Functions and Nonlinear System Design", New York: McGraw Hill, 1968.

[55]   N. Krylov, N. Bogoliubov, "Introduction to Nonlinear Mechanics", Princeton University Press, Princeton, 1947.

[56]   D. P. Atherton, "Nonlinear Control Engineering", Van Nostrand Reinhald Company Limited, 1975.

[57]   M. A. Mahmoud, M. A. A. Kiefa, "Neural Network Solution of The Inverse Vibration Problem", NDT&E International, 32, 91-99, 1998.

[58]   M.–W. Suh, M.–B. Shim, "Crack Identification Using Hybrid Neuro-Genetic Techniwue", Journal of Sound and Vibration, 238,617-635., 2000.

[59]   C. Zang and M. Imregun, "Combined Neural Network and Reduced FRF Techniques for Slight Damage Detection Using Measured Response Data", Archive of Applied Mechanics, 71, 525-536., 2001.

[60]   C. Zang and M. Imregun, "Structural Damage Detection Using ANN and Measured FRF Data Reduced via Principle Component Projection", Journal of Sound and Vibration, 242, 813-827. 2001.

[61]   S. W. Liu, J. H. Huang, J .C. Sung, C. C. Lee, "Detection of cracks using Neural Networks and Computational Mechanics", Computer Methods in Applied Mechanics and Engineering, 191, 2831-2845, 2001.

[62]   J. L. Zapico, M. P. Gonzalez, "Damage Assesment Using Neural Networks", Mechanical Systems and Signal Processing, 17 (1), 119-125, 2002.

[63]   Y.H. Chong, M. Imregun,   "Use of Reciprocal Modal Vectors for Nonlinearity Detection, Archive of Aplied Mechanics, 70, 453-462, 2000.

[64]   G. D. Gounaris, C. A. Papadopolous, "Crack Identification in Rotating Shafts by Coupled Response Measurements", Engineering Fracture Mechanics,69, 339-252, 2002.

[65]   T. C. Tsai, Y. Z. Wang, "Vibration Analysis and Diagnosis of a Cracked Shaft, Journal of Sound and Vibration, 192, 607-620, 1996.

[66]   A. S. Sekhar,   "Vibration Characteristics of a Cracked Rotor wih Two Open Cracks", Journal of Sound and Vibration, 223, 497-512, 1999.

[67]   Y. P. Pu,   "Quasi-Periodic Vibration of Cracked Rotor On Flexible Bearings", Journal of Sound and Vibration, 251, 875-890, 2002.

APPENDIX A

DUAL INPUT DESCRIBING FUNCTIONS

The input to the nonlinearity is taken to be

$$x(t) = B + A\sin(\psi) \tag{A.1}$$

where $\psi = \omega t$; the response of the nonlinearity for this input can be expressed as

$$y(t) = \nu_B B + \nu_A(B + A\sin(\psi)) \tag{A.2}$$

where using Equations (3.38) and (3.39), the DF coefficients ν_B and ν_A can be calculated as follows:

$$\nu_A(A,B) = \frac{1}{\pi A} \int_0^{2\pi} y(B + A\sin(\psi)) d\psi \tag{A.3}$$

$$v_A(A,B) = \frac{1}{\pi A}(\int_0^{\psi_0} m_1(B + A\sin(\psi))\sin(\psi)d\psi$$

$$\int_{\psi_0}^{\pi-\psi_0} m_2(B + A\sin(\psi))\sin(\psi)d\psi +$$ (A.4)

$$\int_{\pi-\psi_0}^{2\pi} m_1(B + A\sin(\psi))\sin(\psi)d\psi)$$

$$v_A(A,B) = \frac{m_1+m_2}{2} + \frac{m_1-m_2}{\pi}(2\frac{B}{A}\cos(\psi_1) + \psi_1 - \frac{\sin(2\psi_1)}{2})$$ (A.5)

and

$$v_B(A,B) = \frac{1}{2\pi B}\int_0^{2\pi} y(B + A\sin(\psi))d\psi$$ (A.6)

$$v_B(A,B) = \frac{1}{2\pi B}(\int_0^{\psi_0} m_1(B + A\sin(\psi))d\psi + \int_{\psi_0}^{\pi-\psi_0} m_2(B + A\sin(\psi))d\psi +$$

(A.7)

$$\int_{\pi-\psi_0}^{2\pi} m_1(B + A\sin(\psi))d\psi)$$

$$v_B(A,B) = \frac{m_1+m_2}{2} + \frac{m_1-m_2}{\pi}(-\psi_0 + \frac{A}{B}(\cos(\psi_0)))$$ (A.8)

Here

$$\psi_0 = a \sin(\frac{\delta - B}{A}) \qquad\qquad (A.9)$$

The above results are valid only for a restricted range of B, $|\delta - B| \leq A$. Outside of this range, N_A is defined as,

$$N_A = m_1 \text{ if } \delta - B > A,$$
$$N_A = m_2 \text{ if } \delta - B < -A. \qquad\qquad (A.11)$$